Accelerator mass spectrometry and its applications

L K Fifield

Department of Nuclear Physics, Research School of Physical Sciences and Engineering, Australian National
University, ACT 0200, Australia

Abstract

The state of the art in accelerator mass spectrometry (AMS) is reviewed. The review is divided
in two parts. The first covers the general methodology, followed by its specific elaborations for
the commonly measured long-lived isotopes such as ^{10}Be, ^{14}C, ^{26}Al, ^{36}Cl and ^{129}I, as well as
other isotopes with emerging applications. The second part considers the very wide spectrum
of applications that now employ AMS, and groups these according to research area rather than
isotope. The period up until late 1998 is covered, with an emphasis on post-1990 developments
and literature.

Contents

1. Introduction

Accelerator mass spectrometry (AMS) is an ultra-sensitive means of counting individual atoms.

Usually, but not invariably, the atoms to be counted are radioactive with a long half-life, and are rare. The archetypal example is ^{14}C which has a half-life of 5730 years and an abundance in living organisms of 10^{-12} relative to stable ^{12}C. Using AMS, the radiocarbon age of a sample less than 10 000 years old can be determined to a precision of 0.5% in a few minutes using a mg or less of carbon. Alternatively, the ^{14}C content can be determined in a sample containing as few as 10^4 atoms of ^{14}C.

The utility of AMS is not limited to ^{14}C alone, however, and many other isotopes are amenable to the technique, the most important of which are ^{10}Be, ^{26}Al, ^{36}Cl and ^{129}I.

AMS emerged from low-energy nuclear physics laboratories in the late 1970s. Its development was driven by a need to radiocarbon-date smaller samples than were possible with the well-known decay-counting method which required about 1 g of carbon. The underlying principles were articulated by Muller (1977) who proposed using a cyclotron as the accelerator and reported the successful detection of ^{3}H. Later in the same year the first AMS observations of ^{14}C from natural materials were reported simultaneously by two groups, one working at McMaster and the other at Rochester (Nelson *et al* 1977, Bennett *et al* 1977). These groups used another type of accelerator, the tandem van de Graaff, which proved to have some powerful advantages over the cyclotron. Subsequently, AMS has been conducted almost exclusively with tandem electrostatic accelerators.

Following these first successful demonstrations, the technique was rapidly embraced by the nuclear physics and ^{14}C-dating communities. This led to the development of the first dedicated AMS systems based on the Mark I Tandetron (Purser *et al* 1980) and the first three were installed at Arizona, Oxford and Toronto in 1981–82. At the same time, several nuclear physics laboratories added an AMS component to their research programs. Techniques for other isotopes, in particular ^{36}Cl (Elmore *et al* 1979), ^{129}I (Elmore *et al* 1980), ^{10}Be (Klein *et al* 1982) and ^{26}Al (Middleton *et al* 1983), were soon developed.

Over the subsequent years, many more accelerators have been given over in whole or in part to AMS and a series of second generation purpose-built systems are now beginning to make their mark. There are presently (1998) about 45 accelerators worldwide which are actively involved in AMS.

In parallel with the growth in the number of facilities, applications of the technique have burgeoned. Traditional ^{14}C-dating is no longer the dominant application. Carbon-14 remains the most important isotope, but much of the research is now directed towards an understanding of global climate change via studies of oceanic circulation, atmospheric processes and past climates. Biomedical applications of ^{14}C are also becoming increasingly important. Cosmic-ray exposure dating, which exploits the build-up of ^{10}Be, ^{26}Al or ^{36}Cl in surface rocks, is making significant contributions to studies of landscape evolution. Beryllium-10 has also been used in studies of soil processes, the deposition of ocean sediments, and the sources of volcanic rocks. Both ^{36}Cl and ^{129}I have been used in hydrology and in tracing the migration of nuclear waste, while ^{26}Al and ^{41}Ca have found application in biomedicine. New applications continue to surface, often spawning new developments in technique.

In this review, the temptation to follow an historical perspective has been eschewed in favour of presenting the current state of the art, particularly in those areas where growth is likely to occur. Accordingly, most of the references are taken from the post-1990 literature, which is not to deny the significance of earlier work, but this has been well covered in earlier reviews (see, for example, Elmore and Phillips 1987, Suter 1990, Kutschera 1990, Finkel and Suter 1993 and the more recent book of Tuniz *et al* 1998; other more specialist reviews are

cited below in the appropriate context).

I have endeavoured to cover as many as possible of the areas of research in which AMS is presently having an impact. Such an approach, however, dictates an economy of discussion. My intent is to signal the significant areas of applications with sufficient detail to allow the reader to delve further. The decision as to what is significant is clearly rather subjective, and I beg the indulgence of those readers who feel that their field has not received the prominence it deserves, or worse, has been omitted altogether.

The first section of the review is devoted to the methodology of AMS. This considers the general principles of the technique, the variety of ways in which these have been implemented, and, since each isotope poses its own particular challenges, the elaborations required for each of the most important isotopes in turn. Applications are treated in the subsequent section, where they are grouped according to field of research rather than by isotope, in the hope that this will be more useful to the reader who wishes to know what AMS can do for his or her field of research.

2. The methodology of accelerator mass spectrometry

2.1. Advantages of AMS

AMS was developed in order to overcome fundamental limitations of both decay-counting and conventional mass spectrometry. These limitations are best illustrated using the familiar example of ^{14}C.

There are 6×10^{10} atoms of ^{14}C in a 1 g sample of modern carbon. Of these, only 14 decay per minute. In order to achieve 0.5% statistical precision with decay counting it would be necessary to count for 48 h. In contrast, typical ^{14}C counting rates in an AMS system are ~ 100 s^{-1}, whence the same precision can be reached in 10 min, and a sample size of 1 mg is all that is required.

A conventional mass spectrometer can in principle count a much higher fraction of the ^{14}C atoms in a sample than decay counting, but in practice the ^{14}C ions are masked by relatively intense fluxes of ions of the ^{14}N isobar, by background from the stable isotopes ^{12}C and ^{13}C, and also by molecular ions such as ^{13}CH, $^{12}CH_2$, ^{12}CD, and $^7Li_2$. Although it is possible in principle to build a mass spectrometer which could resolve these isobaric and molecular interferences, detected ^{12}C currents in such a device would be limited to 1 nA or less, and the corresponding flux of ^{14}C ions would be less than 10^{-2} s^{-1}, i.e. the rate would be comparable to decay counting. In contrast, detected ^{12}C currents in a typical AMS system are ~ 20 μA.

2.2. Principles of AMS

AMS combines the high efficiency of mass spectrometry with excellent discrimination against isobaric and molecular interferences. It achieves this by:

  (i) using negative ions
 (ii) dissociating molecular ions and stripping atomic ions to high positive charge states after a first stage of acceleration
(iii) using a second stage of acceleration followed by identification of individual ions.

Figure 1 shows a schematic representation of an accelerator mass spectrometer. Each of its essential features is described in sequence below. Details specific to individual isotopes will be taken up later.
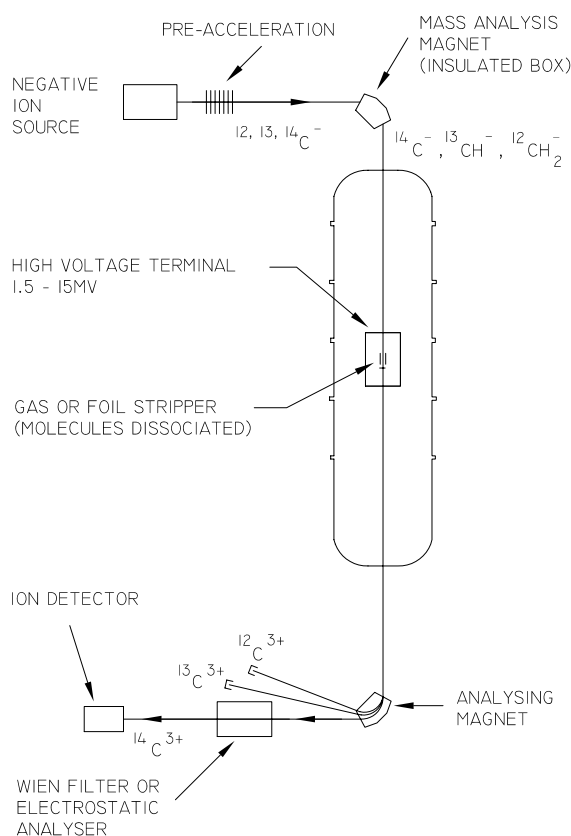
Figure 1. The essential features of an AMS system. The first magnet is shown as transmitting mass-14 negative ions. It is also set periodically to transmit mass-12 and mass-13 ions, in which cases the accelerated ions are detected in the off-axis cups after the analysing magnet.

- Negative ions are generated from the sample in a caesium sputter source, pre-accelerated to 30–200 keV, and mass analysed by a magnet. In the cases of ^{14}C, ^{26}Al and ^{129}I, isobaric interferences are eliminated because ^{14}N, ^{26}Mg and ^{129}Xe do not form stable negative ions.

- The mass-analysed negative ions are accelerated to the positive high-voltage terminal of the accelerator where they encounter either a thin carbon foil or low pressure gas. Several electrons may be stripped off, converting negative atomic ions to multiply charged positive ions, and causing negative molecular ions to dissociate into their component atoms which also emerge positively charged.

- The now positively charged ions are further accelerated back to ground potential in the second stage of the tandem accelerator. A subsequent magnetic analysis selects the ions of interest with a well-defined combination of charge state and energy, and directs them to a detector which generally determines both Z and A of the individual ions. Such positive identification is necessary because ions other than those of the AMS isotope may also reach the detector. For certain isotopes, ^{36}Cl for example, the isobar (^{36}S) readily forms negative ions, and these isobaric ions are potentially the most troublesome because no combination of electric and magnetic fields can prevent them from reaching the detector. Ways of reducing the prohibitively high counting rates that can result will be considered
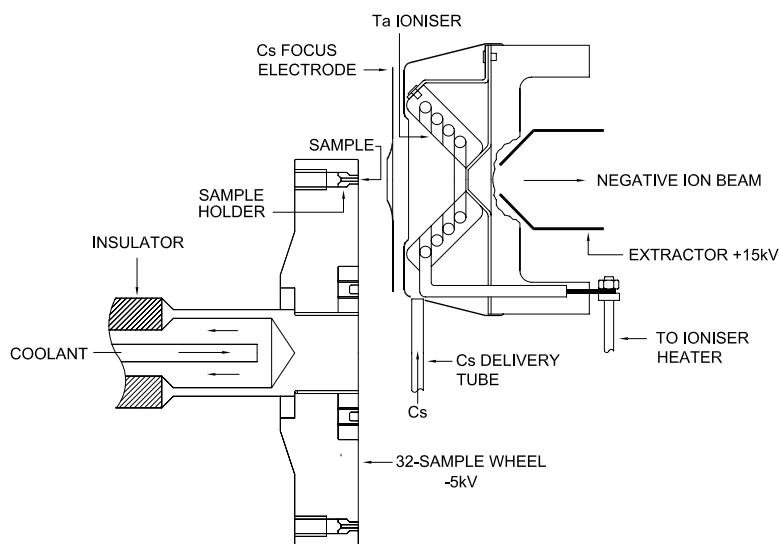
Figure 2. The basic components of a modern (NEC MC-SNICS) high intensity negative-ion source. The ionizer is at local ground potential, and the Cs focus electrode at a voltage intermediate between the ionizer and wheel.

in more detail below in the context of individual isotopes. A fraction of the molecular fragments can also reach the detector as the result of charge-changing collisions with residual gas molecules during the second stage of acceleration. Most AMS systems, therefore, incorporate either a velocity filter or an electrostatic analyser to remove these background ions.

● Generally, AMS determines the *ratio* of the rare isotope to an abundant isotope of the same element, $^{14}C/^{12}C$ for example. This is accomplished by accelerating ions of the abundant isotope or isotopes as well as the rare isotope. Whereas the latter are counted individually, the former (which are typically 10^{12} times more intense) must be measured as an electrical current in a Faraday cup. Various schemes have been devised, and these may be broadly classified into sequential or simultaneous injection methods.

The above gives the bare essentials of an AMS system. In the following, the various components are considered in somewhat more detail.

2.2.1. The ion source. AMS systems based on tandem electrostatic accelerators employ ion sources which utilize a beam of Cs^+ ions to sputter material from the sample. Most laboratories now possess sources which have both the hot tantalum ionizer and the sample within a volume containing Cs vapour. Some of this vapour is ionized on the tantalum surface to create a beam of Cs^+ ions which is focused onto the sample. At the same time, Cs vapour bathes the sample surface where it is available to donate electrons to the sputtered atoms, thereby creating negative ions. Such a source is depicted schematically in figure 2, and typical negative-ion beam currents are given in table 1. More detail may be found in the review of Finkel and Suter (1993).

2.2.2. The injection system. Specialized injection systems have been developed in order to inject both the rare and abundant isotopes into the accelerator.

Table 1. Typical beam currents from high-intensity caesium sputter sources used for AMS.

| AMS isotope	Material	Selected ion of stable isotope	Negative-ion currents (μA)
^{10}Be	BeO	^{9}Be ^{16}O^{-}	1–10
^{14}C	Graphite	^{12}C^{-}	15–60
^{26}Al	Al$_2$O$_3$	^{27}Al^{-}	0.1–1
^{36}Cl	AgCl	^{35}Cl^{-}	5–25
^{129}I	AgI	^{127}I^{-}	2–10

One approach is to inject the different isotopes sequentially, either by changing the energy of the ions prior to mass analysis, or by changing the field in the mass-analysing magnet. The former has the advantage of being fast. Switching times down to microseconds can be achieved by applying a voltage to the electrically isolated vacuum box of the mass-analysing magnet. Electrostatic lenses at the beginning and end of the insulated section are required to ensure identical trajectories of the different isotopes. Many of the dedicated AMS facilities employ this fast-cycling option in order to minimize the effect of fluctuations in the ion source output. Facilities which are shared with nuclear physics research, however, have not in general been modified for fast cycling and are obliged instead to change the field in the mass-analysing magnet. This is a comparatively slow process, although switching times of a few seconds have been achieved even for non-laminated magnets (Perry *et al* 1997).

Beam currents of the stable isotopes can be as high as 100 μA. If injected for more than a few milliseconds, such currents cause the accelerators terminal voltage to drop because the charging system cannot adjust to the increased load. Fast-cycling sequences are chosen to ensure that the intense beam is in the accelerator for a short enough time that this loading is not a problem. At Zurich, for example, the ^{14}C measurement sequence consists of 20 μs, 200 μs and 80 ms on ^{12}C, ^{13}C and ^{14}C, respectively (Suter *et al* 1984a). The Tandetron accelerators can handle larger currents, permitting the use of longer time intervals. At Oxford, the corresponding sequence is 200 μs, 2 ms and 100 ms (Hedges 1984). Laboratories using slow cycling must attenuate the prolific beam before injection into the accelerator with either a beam chopper (Fifield *et al* 1987) or a 'pepper-pot' attenuator (Kubik *et al* 1987).

Alternatively, the stable and radioactive isotopes can be injected simultaneously. Simultaneous injection systems employ a sequence of dipole magnets and lenses which allow the different isotopes to follow different trajectories after leaving the ion source before being recombined at the entrance to the accelerator. This approach was pioneered at McMaster (Southon *et al* 1990) and has been adopted for the Mark II Tandetron systems (Purser *et al* 1990). The recombinator for the latter machines, which are used almost exclusively for ^{14}C, is depicted in figure 3. Attenuation of the intense ^{12}C beam is accomplished by interposing a rotating slotted wheel in its path where the separation of the isotopes is a maximum.

2.2.3. The accelerator. The tandem electrostatic accelerators employed in AMS may be conveniently grouped into three categories on the basis of their maximum terminal voltage, V_{T}.

(i) $V_{\mathrm{T}} < 3$ MV. This category includes the Marks I and II tandetrons, and more recently, small machines from the National Electrostatics Corporation (NEC). They are predominantly used for high-precision ^{14}C measurements, but also for ^{10}Be, ^{26}Al and ^{129}I, and typically operate at $\sim$2.5 MV. The tandetrons are charged by a radio-frequency voltage-doubling power supply.
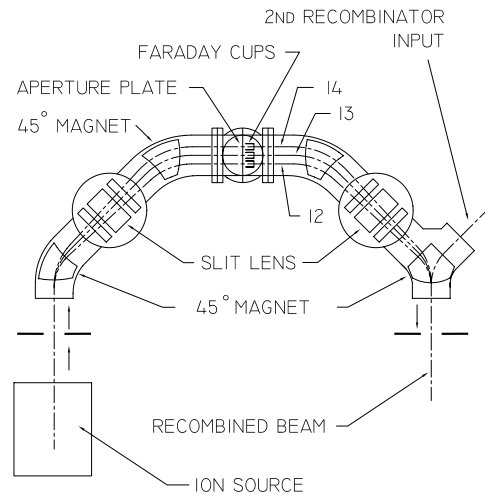
Figure 3. The recombinator injection system used by the AMS systems based on the Mk II Tandetrons.

(ii) $4.5 < V_T < 9$ MV. Machines in this category are principally extensively modified ex-nuclear physics accelerators, predominantly model-EN and FN accelerators manufactured by High Voltage Engineering Corporation in the 1960s and 1970s. Recently, NEC have delivered three purpose-built 5 MV machines to the University of Tokyo and the National Institute for Environmental Studies (Tsukuba) in Japan and York University in the UK. The full range of AMS isotopes can be covered by accelerators of this size.

(iii) $V_T > 10$ MV. These are operational nuclear physics accelerators on which AMS typically takes 20% of the beam time. Modifications to the injection system or accelerator specifically for AMS are usually minimal. The higher energies available from these larger machines are advantageous for ^{36}Cl, and in addition, much of the development of new isotopes has been carried out on them. They include the NEC 14UD Pelletron and HVEC MP and XTU accelerators.

The desirable criteria for an AMS accelerator are that transmission of ions through the accelerator should be high and reproducible, that this transmission should be insensitive to small changes in the injection or accelerator parameters, and that the terminal voltage should be very stable. High and flat-topped transmission is achieved by using large-diameter acceleration tubes, spacious vacuum chambers within magnets, and apertures which are as large as possible. Consistency of transmission is best achieved using gas stripping in the high-voltage terminal, and most of the facilities which aim at high precision ^{14}C use an argon gas stripper. Gas stripper canals are typically 8 mm in diameter and may constitute the smallest restriction in the system. Careful attention to ion optics is therefore required to ensure that transmission losses are minimal.

Stabilization of the accelerator's terminal voltage presents a particular challenge. The usual slit-stabilization method, which depends on nA currents striking slits after the final analysing magnet, is not applicable since there are typically only a few ions per second of the AMS isotope. Two solutions have been adopted. Either the signal from a generating voltmeter (GVM) is used, or the off-axis position of one of the stable beams is monitored by a Faraday cup which is split in two to give separate left and right signals (Suter *et al* 1984b). The former is the more widely used and is capable of excellent stability. For example, fluctuations in the

terminal voltage of the 14 UD accelerator at the Australian National University are ~1 kV in 14 MV under GVM stabilization. Of course, it helps if the accelerator is intrinsically very stable, and pelletron or laddertron charging systems have distinct advantages over rubberized belts in this regard.

2.2.4. Post-acceleration analysis. Following acceleration, the charge state and hence energy of interest is selected by magnetic analysis. In those systems employing fast cycling or simultaneous injection, the radii of curvature of the AMS isotope and the stable isotopes are different, and the latter are collected in off-axis Faraday cups after the magnet. Evidently, the width of the magnet poles and of the vacuum box at the exit from the magnet must be sufficient to accommodate the different ion species. For example, the separation between ^{12}C and ^{14}C is 8 cm at the exit from a typical 1 m radius analysing magnet. This is rather more than is found on analysing magnets installed on nuclear physics accelerators, and costly modifications or a new magnet are required if fast cycling is to be implemented. In general, these modifications have been implemented on the EN and FN conversions, but not on the larger machines.

Most systems employ an additional analysis stage, consisting of an electrostatic analyser or a velocity filter, to remove that small fraction of molecular fragments which has acquired the correct energy to follow the same trajectory as the AMS isotope through the analysing magnet. These can otherwise cause unacceptably high counting rates in the ion detector. Rates depend on the vacuum in the high-energy tube, and because some unwanted ions inevitably leak through the additional analysis stage, the higher the vacuum the better. To this end, gas strippers which employ turbo-molecular pumps to recirculate the gas (Bonani *et al* 1990) are now widely employed. In addition, acceleration tubes of the NEC design, in which ceramic insulators are bonded without adhesives to titanium electrodes, offer advantages in terms of higher vacuum over the more widely used tubes in which glass insulators are bonded to metal electrodes with organic adhesives.

2.2.5. Detectors. A range of ion detectors have been variously employed to count the AMS isotope.

Silicon detectors

These measure only the energy of the ion. In some cases, this is sufficient for unique identification of the AMS isotope. A drawback of silicon detectors is that they are susceptible to radiation damage.

Ionization chambers

Ionisation chambers provide not only a measure of the total energy of an ion, but also its rate of energy loss as it slows in the detector gas. They are also more robust than silicon detectors. A typical multi-element ionization chamber is depicted in figure 4. The gas-confining window is usually of Mylar, typically 1.5 μm thick. Propane or isobutane is normally employed as the counter gas. The latter has the advantage of a higher stopping power but is comparatively expensive, while the former is cheap and readily available. Electrons produced by the passage of the energetic ion drift towards the anode in the transverse electric field. The anode is subdivided into sections, each of which collects those electrons produced beneath it, thereby measuring the energy lost by the ion along that portion of its track. Since ions of different Z lose energy at different rates, this energy-loss information permits the separation of isobars,
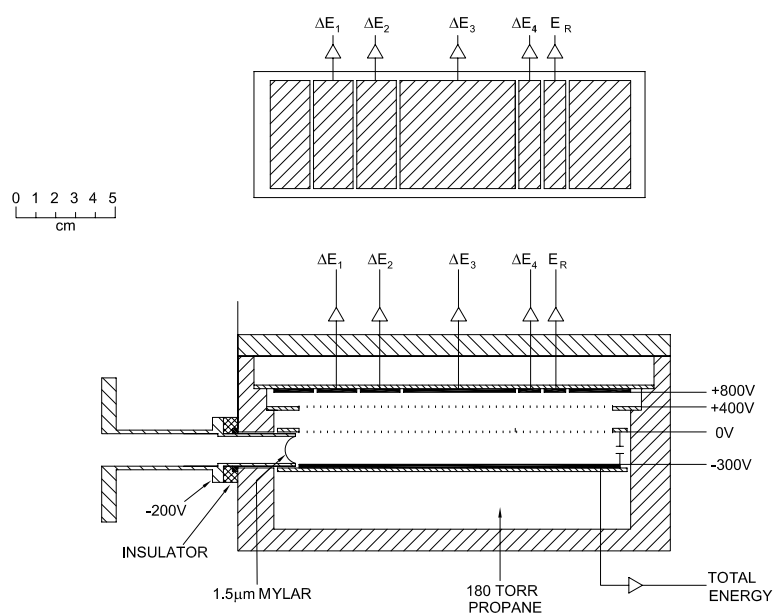
Figure 4. A cross section through the multi-element ionization chamber used at the Australian National University for [36]Cl, ^{14}C and [26]Al detection. The upper panel shows a plan view of the anode electrode.

[36]Cl and [36]S for example, which have identical energies when they arrive at the detector. Issues specific to certain isotopes will be taken up in section 3 below.

Bragg-curve detectors, in which the electric field is parallel to the ion track, are also in use in some AMS laboratories. In these detectors, the energy-loss information is obtained from the time development of the signal at the anode.

Hybrid detectors, which employ a gas ionization chamber for energy-loss measurement and a silicon detector to measure the residual energy, are also used (Middleton *et al* 1983, Boaretto *et al* 1990).

Time-of-flight systems

For heavier ions, the energy resolution of an ionization chamber or silicon detector is often insufficient to resolve neighbouring masses. Better separation is possible by combining the energy measurement with a determination of the ions velocity via a time-of-flight measurement. Such systems are widely used for [129]I, and have also been used for other isotopes.

A time-of-flight system consists of 'start' and 'stop' detectors separated typically by 2 m. Start detectors invariably consist of a thin carbon foil and a microchannel plate which multiplies the electrons liberated from the foil by the passage of the ion. Considerable ingenuity has been exercised in ensuring that the electron collection is isochronous, with electrostatic mirrors, deflectors or uniform magnetic fields variously employed to direct the electrons to the microchannel plate. The stop detector may be similar to the start detector, in which case it is backed by a silicon detector or ionization chamber for energy measurements. Alternatively, a silicon detector (which may be part of a hybrid system) is often used to provide both timing and energy signals. Typical time resolutions achieved with such devices are 300–500 ps, which is more than adequate to separate [129]I from [128]Te and [127]I as illustrated in figure 5.
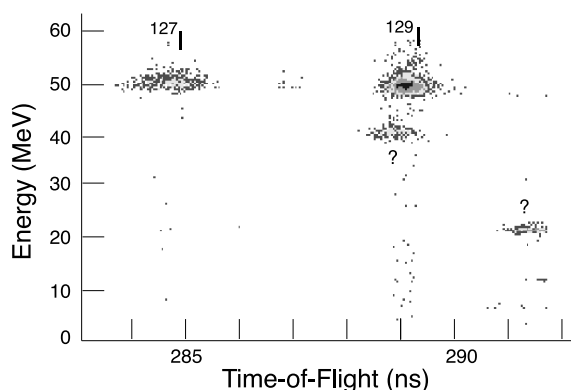
Figure 5. An energy versus time-of-flight spectrum obtained with the Chalk River detection system showing the clear separation of ^{129}I from other ion species. ^{127}I and ^{129}I are separated by 4.5 ns. A few ^{128,130}Te counts are visible between the iodine peaks. Peaks labelled '?' have not been identified. (From Koslowsky *et al* 1997.)

A drawback of time-of-flight systems is the loss of efficiency associated with scattering from grids and from the start foil, and efficiencies typically range between 50 and 80%. Scattering from the foil is crucially dependent on the foil thickness, and carbon foils as thin as 2 μg cm^{-2} are necessary for optimum transmission. The Chalk River group have experimented with thin diamond films (Koslowsky *et al* 1997) which may have advantages in this regard.
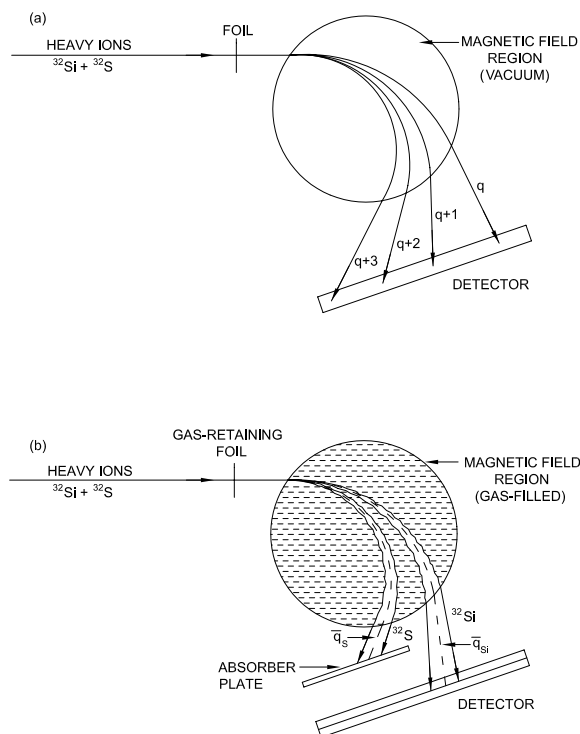
Gas-filled magnets

Isobars, which have the same mass and energy after acceleration, may be separated by passing them through a gas-filled region within a magnetic field. Because the isobars have different Z, their average charge states are different in the gas-filled region, and hence they follow different trajectories in the magnetic field as illustrated in figure 6. Provided that the ions undergo a sufficient number of collisions with the atoms of the gas, and pressures of a few torr ensure that this condition is met, the trajectories may be sufficiently well-defined to permit a spatial separation of the isobars at the exit from the magnetic field region where the unwanted, high counting-rate isobar can be intercepted by an appropriately-positioned baffle. The AMS isotope continues to an ionization chamber which distinguishes between the AMS isotope and events due to tails of the isobar distribution. An excellent review of gas-filled magnets as applied to AMS has been given by Paul (1990).

Design criteria for an optimised gas-filled magnet system are discussed by Zoppi (1993), and purpose-built systems have been installed at Zurich (Zoppi *et al* 1994) and Munich (Knie *et al* 1997). Existing magnetic spectrometers have also been pressed into service (Korschinek *et al* 1994, Popplewell *et al* 1998).

X-ray detectors

It is possible to identify fast elemental ions by the characteristic x-rays they emit following excitation in a foil, allowing isobar separation at energies where ionization chambers give rather poor discrimination. Application of this technique to AMS was first demonstrated at Toronto (Artigalas *et al* 1994), and subsequently developed at Zurich (Wagner *et al* 1994, 1995) and

Figure 6. Principle of the gas-filled magnet for the separation of isobars. (*a*) In the absence of gas, ions with a range of charge states are produced by passage through a foil, and give rise to a series of sharp peaks along the focal plane of the magnetic spectrometer which are the same for the two isobars. (*b*) In the presence of gas, the isobars follow different average trajectories which are determined by Z. Fluctuations about the average trajectory produce much wider 'peaks' at the detector, but the separation of the isobars may be sufficient to allow the high-counting rate one to be intercepted before the detector. (After Paul 1990.)

Livermore (McAninch *et al* 1995, 1997). It has been applied to the detection of several isotopes including ^{36}Cl, ^{59,63}Ni, ^{60}Fe, ^{79}Se and ^{126}Sn. The optimal foil material has $Z_{foil} \approx Z_{ion} + 2$, and x-ray yields are strongly dependent on energy. At the energies obtainable from a 7 MV accelerator, yields vary from one x-ray per incident ion for light ions such as Si to one x-ray per 300 incident ions for ^{106}Pd. Only a small fraction of these x-rays are actually detected, however, due to the limited solid angle subtended by the detector and an intrinsic detector efficiency of less than unity. Because there is no discrimination between different isotopes of the same element, an initial time-of-flight measurement is required to distinguish between, for example, ^{59}Ni and any ^{58}Ni or ^{60}Ni that reach the detector.

3. Techniques for individual isotopes

3.1. Carbon-14 ($T_{\frac{1}{2}} = 5730$ a)

Applications of ^{14}C place more stringent demands on precision than those of any other isotope, and a precision of 0.5%, corresponding to 40 years in radiocarbon age, is the aim of the dedicated or semi-dedicated AMS laboratories. In order to attain this level of precision it is necessary, first to obtain sufficient ^{14}C counts that the statistical uncertainty is at the desired

level, and second to achieve a high degree of reproducibility. These dual requirements are being met as follows:

(i) Most laboratories employ high-current, multiple-sample ion sources with graphite as the sample material. Although the modern commercial sources (HVEE 846 and NEC MC-SNICS) are capable of delivering up to 100 μA of $^{12}C^-$, many laboratories prefer to operate at $\sim$25 μA, principally to avoid the effects of space charge on the emittance of the beam, but also to prolong the period between cleanings. The group at the Lawrence Livermore laboratory, however, routinely operate their extensively modified type-846 source at outputs of 50–100 μA. Because measurements are made relative to a standard which is counted for about the same length of time as the unknown sample, 60 000 counts are required for a statistical accuracy of 0.5%. A 5000 year-old sample gives a ^{14}C counting rate of $\sim$35 s^{-1} at a source output of 25 μA. Samples must therefore be run for a total of 20–30 min to obtain the requisite number of counts. At Oxford, a source which uses CO_2 rather than graphite has been in operation for several years (Bronk and Hedges 1990, 1994, 1997). In this case, the disadvantage of lower beam currents ($\sim$10 μA) is compensated by the substantial simplification in sample preparation.

(ii) Cratering of the sample as sputtering progresses can lead to changes in emittance and hence to isotope-dependent changes in transmission. In the type-846 source, cratering is avoided by moving the sample around under the caesium beam. Although the MC-SNICS does not have this capability, the Arizona laboratory has nevertheless achieved precisions of 0.3% using the first of these sources (Donahue *et al* 1997).

(iii) Excellent ion–optical transmission and insensitivity to small changes in any of the system parameters is required for high precision. Transmissions for the dedicated ^{14}C systems are typically >80%.

(iv) Argon gas stripping is generally employed to avoid the variations in foil thickness that foil stripping is prone to, as well as to reduce losses due to scattering.

(v) Either fast-cycling or simultaneous injection is required to ensure that the measured isotope ratios are independent of variations in the ion–source output. Simultaneous injection is employed by the Mark II Tandetron systems at Woods Hole, Groningen and Kiel, and a variant is also employed by the Tokyo group (Kobayashi *et al* 1990a). Fast cycling is employed in the Mark I Tandetron systems, in the EN and FN conversions, and in the NEC systems delivered to Tokyo, Tsukuba and Vienna.

(vi) A high level of automation is required to control not only the fast-cycling sequence (if employed), but also the sequencing of samples with appropriate interleaving of unknowns and standards and, usually, multiple runs on any given sample. In addition, the computer control program often maintains a watch on the integrity of the data by continuously monitoring the ratios of the different isotopes as a measurement proceeds. Possible problems can then be identified and flagged for later consideration, or an operator can be alerted.

(vii) For high-precision dating, it is necessary to correct for the natural fractionation inherent in biological processes. For example, carbon from C3 plants (e.g. forest trees), is depleted by 1.5% in ^{13}C relative to C4 plants (most grasses). Hence, in addition to the AMS measurement of the $^{14}C/^{12}C$ ratio, a measurement of the $^{13}C/^{12}C$ ratio is also required. Usually the $^{13}C/^{12}C$ ratio is measured with a conventional mass spectrometer on a subsample of CO_2. Some laboratories, most notably Zurich (Wölfli 1990), achieve sufficient precision ($\sim$0.2%) in the AMS measurement of the $^{13}C/^{12}C$ ratio to be able to avoid this extra step. This approach also has the advantage of accounting for any additional fractionation introduced in the graphitization process.

Table 2. Typical operational parameters for ^{10}Be measurements.

Accelerating voltage	Stripping	Charge state	Energy	^{10}B reduction	Reference
2 MV	gas only	2$^+$	5 MeV	differential energy loss in external foil	Raisbeck *et al* (1984)
6 MV	gas + foil	3$^+$	20 MeV	complete absorption of ^{10}B in gas cell	Klein *et al* (1982)

3.2. Beryllium-10 ($T_{\frac{1}{2}} = 1.50$ Ma)

Beryllium does not form a stable negative atomic ion. Samples are therefore prepared as beryllium oxide and the BeO$^-$ ion is selected for analysis. Currents of several microamps are obtained from modern high-intensity sources.

Two consequences attend the use of molecular ions. First, the ^{10}Be atom carries only $\frac{10}{26}$ of the energy of the molecular ion at the terminal stripper and hence strips to a lower average charge state than if it had the full energy. Secondly, if only a foil stripper is used, substantial losses are incurred due to 'Coulomb explosion' of the molecule. The strong electric repulsion between the Be and O atoms immediately after they have been stripped of several electrons in the foil while still effectively at the molecular separation adds both longitudinal and transverse components to the momenta of the ions. Losses result from the increased divergence of the beam, and from an energy spread (60 keV for Be^{3+} ions at an accelerating voltage of 8 MV) which exceeds the acceptance of the post-acceleration analysis system. A gas stripper, because it dissociates the molecule more gradually by stepwise removal of electrons, minimises these effects. The combination of the two, where a low-pressure gas stripper precedes a foil, minimises Coulomb explosion while retaining the advantage of a higher average charge state, and this configuration is generally used at those laboratories with the larger accelerators. Gas-only stripping is used by the smaller accelerators, however. Representative parameters employed at various laboratories for ^{10}Be measurements are collected in table 2.

Boron-10 is the stable isobar of ^{10}Be, and since the BO$^-$ ion is formed as readily as the BeO$^-$ ion, ^{10}B ions accompany the ^{10}Be ions after acceleration. Despite the best efforts of the chemist, counting rates of these unwanted ^{10}B ions are generally well beyond the capabilities of ionization detectors. Two solutions to this problem have been adopted, depending upon whether the accelerator is large ($\geqslant$5 MV) or small ($\sim$2 MV).

(i) At the final energies of 20 MeV or more achieved with the larger accelerators, the difference in range of ^{10}B and ^{10}Be ions is such that a ^{10}Be ion still has $\sim$40% of its initial energy after ^{10}B has been brought to a halt. Hence, the ^{10}B ions may be stopped in a gas cell or a foil before the detector, while the ^{10}Be ions continue on to deposit their residual energy in the detector. Discrimination between ^{10}Be ions and other species such as ^{9}Be and ^{7}Be may be improved by deriving two or more energy loss signals.
Because ^{7}Be ions from the ^{1}H(^{10}B, ^{7}Be) ^{4}He reaction can constitute a serious background when ^{10}B fluxes are high, it is necessary to avoid any hydrogenous component of the gases and windows of the absorber cell and the detector. Argon is usually used in the gas-absorber cell, freon-14 (CF$_4$) in the detector, and havar (a Co/Cr/Fe/Ni/W alloy) is used for the first window. An advantage of using a gas cell as the ^{10}B absorber is that it may be configured as an ion chamber. A ^{10}B flux of 10^6 s^{-1} produces an ion current of $\sim$100 nA, which can be used to tune the AMS system for optimal ^{10}Be transmission.
A variant of the gas-cell approach, in which the absorption region is incorporated into the detector itself, has been developed at the Australian National University (Fifield *et al* 1990)
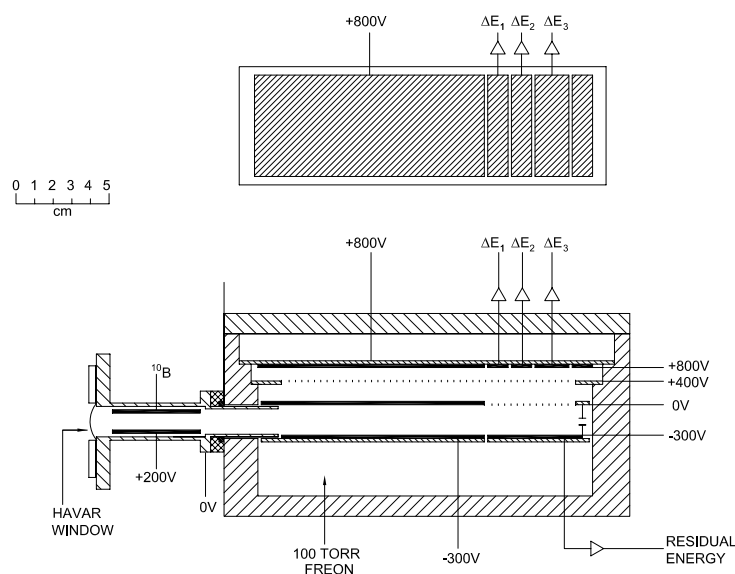
Figure 7. The ^{10}Be detector used at the Australian National University. It incorporates the stopping of ^{10}B and the measurement of the residual energy of ^{10}Be within the same gas volume.

and is depicted in figure 7. This approach dispenses with two foils and a separate gas-handling system. In order to decouple the rear, ^{10}Be-measuring section of the detector from the front, ^{10}B-stopping section, there are separate front and rear cathodes, and electrons produced by ^{10}B ions are prevented from reaching the anode plane by a solid metal plate in place of a grid. A pair of plates near the entrance window function as an ion chamber to measure the ^{10}B flux as described above. At ^{10}B (and ^{10}Be) energies of 27 MeV, no cross-talk between the front and rear sections of the detector is observed at ion chamber currents up to several μA.

(ii) At the lower energies available from the Tandetrons, it is not possible to use the total absorption technique because the straggling in the range of 5 MeV ^{10}B ions is too large. The 'small-accelerator' solution is to interpose a 200 μg cm^{-2} carbon foil in the path of the ions before the final magnetic analysis (Raisbeck *et al* 1984). On average, ^{10}B ions lose 300 keV more energy in this foil than the ^{10}Be ions and hence all but 0.2% of them are rejected by the final magnetic analysis. ^{10}Be ions are also lost due to energy straggling and because they emerge from the foil in a range of charge states, and typically only 20% of them reach the detector. Nevertheless, the counting rate of ^{10}B ions is diminished by a factor of 100 relative to ^{10}Be, and more importantly, the ^{10}B rate is decreased to a level that can be handled by an ionization counter. In this case, the full energy of the ions is deposited in the detector, and ^{10}Be and ^{10}B ions may be distinguished by subdividing this into energy loss and residual energy signals.

The ^{10}Be/^{9}Be ratio can be determined either by injecting ^{10}BeO$^-$ and ^{9}BeO$^-$ sequentially, or by a novel simultaneous injection method (Middleton and Klein 1987a). The latter exploits the fact that ^{10}Be ^{16}O$^-$ and ^{9}Be ^{17}O$^-$ are injected into the accelerator simultaneously and that, after acceleration, ^{17}O^{5+} ions differ by only 1% in magnetic rigidity from ^{10}Be^{3+} ions. Hence, the ^{17}O^{5+} ion current, which is a surrogate for the ^{9}Be current, can be collected continuously in an off-axis Faraday cup after the post-acceleration analysing magnet, even for magnets which do not have large-acceptance vacuum boxes (see section 2.2.4).
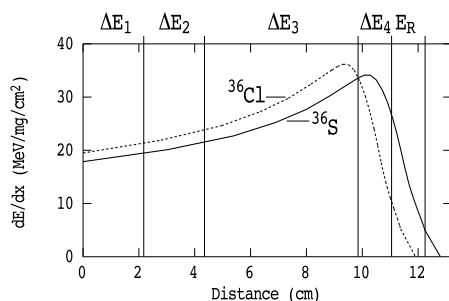
Figure 8. Energy loss as a function of distance into a gas-ionization counter for 154 MeV ^{36}Cl and ^{36}S ions. The positions of the anode electrodes of the detector shown in figure 4 are indicated.

3.3. Chlorine-36 ($T_{\frac{1}{2}} = 301$ ka)

The ^{36}S isobar is the principal challenge confronting AMS measurement of ^{36}Cl. Sulfur forms negative ions as readily as chlorine, and although ^{36}S constitutes only 0.02% of natural sulfur, a mere 1 ppm of sulfur yields a ^{36}S counting rate which is three orders of magnitude higher than the ^{36}Cl rate from a typical environmental sample with ^{36}Cl/Cl $\sim 10^{-13}$. Since 0.1–1 ppm sulfur contamination is typical and a sensitivity of 10^{-15} in the ^{36}Cl/Cl ratio is desirable, the detector must be capable of discriminating between ^{36}Cl and ^{36}S ions when the latter are 10^5 times as intense as the former and are counting at 1000 s^{-1}.

Such discrimination requires the higher energies available from the larger accelerators. Effective separation between ^{36}S and ^{36}Cl is best achieved if the maxima in the rates of energy loss (the Bragg peaks) for the two species occur at rather different distances into the detector. At energies above the Bragg peak, i.e. >24 MeV, there is a ~13% difference in energy loss between ^{36}Cl and ^{36}S, which, if accumulated over a sufficient distance in the detector gas, leads to a substantial spatial separation of the Bragg peaks as illustrated in figure 8 for 154 MeV ions. In a detector such as that shown in figure 4, this spatial separation results in large differences between ^{36}S and ^{36}Cl in particularly the E_R and ΔE_4 signals as shown in figure 9. The other ΔE signals also provide useful discrimination, and the resulting high degree of redundancy in ion identification allows the rejection of ^{36}S ions with a rejection ratio of better than 10^6:1 at counting rates up to 10^4 s^{-1}. Other ion species, which have different energies from ^{36}Cl, are readily distinguished via a total energy signal derived from the coupled cathode and grid electrodes.

Chlorine-36 is also measured routinely at several laboratories using FN and even EN accelerators where the available energies are significantly lower than the 150 MeV in the example above.

At PRIME Lab, measurements are conducted with 56 MeV ^{36}Cl^{7+} ions. Tight gating of the spectra from a detector similar to that shown in figure 4 allows adequate separation between ^{36}Cl and ^{36}S ions at ^{36}S counting rate up to 1000 s^{-1} (Knies and Elmore 1994). Discrimination against the troublesome background arising from large angle scattering of a small fraction of the ^{36}S ions in the detector gas is enhanced by using the relative arrival times of the electrons at the front and back anode electrodes as an additional parameter.

At Zurich, measurements are conducted with 48 MeV ^{36}Cl^{7+} ions (Synal *et al* 1994). The detection system is again a multi-anode ionization chamber, which suppresses ^{36}S relative to ^{36}Cl by a factor of 2×10^4. Ions of the stable chlorine isotopes are not well resolved from ^{36}Cl by the detector and must be prevented from reaching it by electrostatic analysers at both the low- and high-energy ends of the system. Both Purdue and Zurich report ^{36}Cl/Cl sensitivities of ~10^{-15} provided that the ^{36}S rates are suitably low.

In order to achieve effective sulfur concentrations of <1 ppm, it is necessary both to
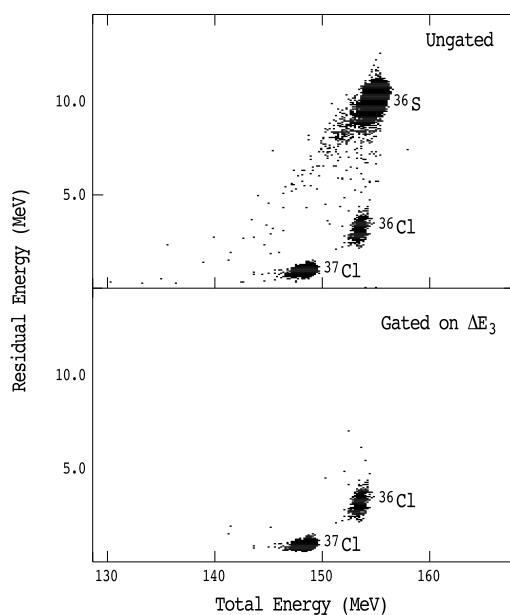
Figure 9. Bi-dimensional plot of residual energy versus total energy showing the separation of 154 MeV ^{36}Cl and ^{36}S ions. The lower plot was obtained after applying a gate on the ΔE_3 signal which accepted chlorine, but not sulfur, ions. The ^{36}Cl/Cl ratio of the sample was 430×10^{-15}.

purify the sample to remove sulfur, and to ensure that any parts of the sample holder that can be sputtered by the caesium beam are also very low in sulfur. The former is accomplished by a chemical procedure described by Conard *et al* (1986), while the latter is achieved by masking any exposed surfaces with either silver bromide or the sample itself.

3.4. Aluminium-26 ($T_{\frac{1}{2}} = 720$ ka)

AMS of ^{26}Al is technically more straightforward than ^{36}Cl because the ^{26}Mg isobar does not form a stable negative ion. The principal limitation arises from the reluctance of aluminium to form negative ions due to its low electron affinity (0.44 eV). Middleton and Klein (1987a) report typical currents of 2 μA of Al$^-$ from Al$_2$O$_3$ samples, and similar currents are obtained at Livermore, but 0.2–0.5 μA seems to be more typical at other laboratories. Consequently, and especially for geological samples which have ^{26}Al/Al ratios of less than 10^{-13}, running times per sample tend to be long, and measurement precision low. Generally, the insulating Al$_2$O$_3$ is mixed with an approximately equal weight of silver powder to ensure good electrical and thermal conduction.

Representative operating conditions for ^{26}Al at various laboratories are summarized in table 3. An odd charge state is employed in all cases. If an even charge state such as ^{26}Al^{6+} is selected, intense counting rates of ^{13}C^{3+} (from the injection and subsequent breakup of the ^{13}C$_2^-$ molecular ion) are observed. These ions have the same E/q and mE/q^2 as ^{26}Al^{6+} and therefore pass all magnetic and electric analysers.

The AlO$^-$ ion is produced an order of magnitude more prolifically than the Al$^-$ ion from Al$_2$O$_3$ samples. It suffers, however, from the drawback that MgO$^-$ ions are also formed in the ion source, and count rates of ^{26}Mg ions at the detector are generally prohibitively high if the AlO$^-$ ion is selected for injection. It is possible to eliminate ^{26}Mg ions by fully stripping to Al^{13+} after acceleration, but this approach requires a very large accelerator in order to achieve significant yield of fully stripped ions. It was pioneered at the Daresbury laboratory (Barker *et al* 1990), but has not been adopted elsewhere.

Table 3. Representative operational parameters for ^{26}Al measurements.

Accelerating voltage	Stripping	Charge state	Energy	Reference
2 MV	gas only	3^+	8 MeV	Yiou *et al* (1986)
7.5 MV	foil	7^+	60 MeV	Middleton *et al* (1983)
11.4 MV	foil	7^+	91 MeV	King *et al* (1997b)

3.5. Iodine-129 ($T_{\frac{1}{2}} = 15$ Ma)

Since ^{129}Xe does not form a stable negative ion, AMS of ^{129}I is not troubled by the stable isobar. Consequently, ^{129}I can be measured as effectively with a small accelerator as with a large one (Kilius *et al* 1987). Several μA of iodine beam can be obtained from AgI samples and sensitivities $\sim 10^{-15}$ in the ^{129}I/^{127}I ratio are readily achievable.

The most serious background arises from ^{127}I ions. A very small fraction of the ^{127}I$^-$ ions produced in the ion source may have sufficient additional energy, acquired from the sputtering Cs$^+$ beam, to be injected along with the ^{129}I ions. Their contribution can be minimized by sputtering with low energy, typically 2 keV, Cs$^+$ ions. Systems which employ pre-acceleration to ~ 100 keV before the magnetic mass analysis enjoy an additional advantage. At this energy, an ^{127}I ion must acquire 0.8 keV from the Cs$^+$ beam in order to have the same magnetic rigidity as an ^{129}I ion, whereas at the ~ 20 keV characteristic of the smaller accelerators, only an additional 0.16 keV is required. Since the probability of energy transfer, δE, decreases as $\sim 1/(\delta E)^2$, the number of injected ^{127}I$^-$ ions is reduced by a factor of ~ 25 at the higher pre-acceleration energy.

Alternatively, the 'sputter tail' can be eliminated almost entirely by adding an electrostatic deflector to perform an energy analysis between ion source and mass-analysis magnet. This is essential if ^{129}I is to be measured on small accelerators, and following Toronto's lead (Kilius *et al* 1987), several laboratories have installed such devices.

Gas stripping is generally preferred for ^{129}I because losses due to multiple scattering are significantly less than in a foil. Foil stripping is, however, employed by the group working at the 14UD accelerator of the Weizmann Institute, who operate at 11.8 MV with the 11$^+$ charge state (Paul *et al* 1987a).

At the small machines, the discrimination achieved by the combination of electrostatic deflectors at both the low- and high-energy ends of the accelerator is sufficient to ensure that the only ions arriving at the detector with the correct charge state are ^{129}I. Ions with different charge states have significantly different energies and hence a detector with only modest energy resolution is all that is required.

On the larger machines, which generally lack a pre-injection electrostatic deflector, time-of-flight detection systems are widely employed to separate ^{129}I from those ^{127}I ions which elude the high-energy electrostatic analysis. Under the favourable conditions of both high injection energy and high vacuum in the accelerator tubes, a single energy measurement may, however, be all that is required (Fifield *et al* 1994, Sharma *et al* 1997).

3.6. Calcium-41 ($T_{\frac{1}{2}} = 103$ ka)

AMS of ^{41}Ca requires the injection of a molecular ion because, although the Ca$^-$ ion is stable, its binding energy is so low that it is formed with very low probability in sputter sources. CaH$_3^-$ has generally been the ion of choice. Beam currents of several μA can be obtained from solid calcium hydride (Fink *et al* 1990a), and the choice of the tri-hydride ion eliminates the ^{41}K

isobar because the KH_3^- ion is not stable. Unfortunately, the production of CaH_2 requires the time-consuming *in vacuo* reduction of CaO to calcium metal.

Alternatively, the CaF_3^- ion may be used since, like KH_3^-, the KF_3^- ion is unstable. The starting material is CaF_2 which is very much simpler to produce than CaH_2. Simplicity of sample preparation is, however, offset by the disadvantages of lower beam currents, a more extensive suite of molecular fragments, and lower final energy, and most laboratories that have made ^{41}Ca measurements have therefore opted for the hydride ion. The Lawrence Livermore Laboratory has been the principal exception (Freeman *et al* 1995, Freeman and Vogel 1995). Their interest is in biomedical applications where the potential number of samples is large and hence simplicity of sample preparation is particularly attractive.

In the absence of the ^{41}K isobar, detection of ^{41}Ca is straightforward, and the multi-element ionization chambers used for ^{36}Cl and ^{26}Al are very suitable.

3.7. Actinides

Using their heavy-element beam line, which was constructed principally for ^{129}I measurements and the assay of platinum-group elements (section 4.11), the Toronto group have reported the detection of ^{232}Th (Kilius *et al* 1990) and ^{244}Pu (Zhao *et al* 1994a), and demonstrated the occurrence of ^{236}U in high-grade uranium ore at a $^{236}U/^{238}U$ ratio of 2×10^{-10} (Zhao *et al* 1994b). Purser *et al* (1996) have taken the concept further, discussing the design principles of a system specifically for the measurement of actinide elements. Uranium-236 presents the greatest challenge, because the beam analysis system must completely eliminate ions of the stable uranium isotopes (which are many orders of magnitude more abundant in the sample material) since the detection system does not provide any effective discrimination between ^{236}U and ^{235}U.

A different approach, applicable to the long-lived plutonium and neptunium isotopes, but not to ^{236}U, has been pursued at the Australian National University (Fifield *et al* 1996, 1997). In this approach, all of the isotopes are counted as individual ions in an ionization chamber. Normalization is provided by a few pg of ^{242}Pu which is added to the sample prior to chemical processing, and the ratios of ^{239}Pu and ^{240}Pu to ^{242}Pu are determined by AMS. Sample preparation consists of extraction of the plutonium in a sample on an ion-exchange column, followed by dispersal of the plutonium in ~ 2 mg of iron oxide to provide sufficient bulk for the ion source. Molecular PuO^- ions are selected from the ion source in preference to the more weakly formed Pu^-, and a low-pressure gas stripper is employed. At present, the operating voltage of the accelerator is limited to 4.3 MV by the bending power of the energy-analysing magnet for Pu^{6+} ions. A longitudinal-field ionization chamber with an energy resolution of 3% for ~ 30 MeV actinide ions provides excellent discrimination against lower-mass ions arriving at the detector. Sensitivities of 10^6 atoms have been achieved for $^{239,240,242,244}Pu$ and ^{237}Np. For ^{239}Pu, this is two orders of magnitude better than α-particle counting.

3.8. Other isotopes

Techniques have been developed for the measurement of several other isotopes, but none of these has yet found wide application. For completeness, each is considered briefly below.

3.8.1. ^3H ($T_{\frac{1}{2}} = 12$ a). Decay counting is a very sensitive method for the detection of tritium due to its short half-life. Nevertheless, AMS offers the advantage of smaller sample size, particularly in biomedical applications. A tritium capability has been developed on the Lawrence Livermore system (Roberts *et al* 1994).

3.8.2. ^{32}Si ($T_{\frac{1}{2}} = \sim 160$ a).   Silicon-32 is produced in the atmosphere by spallation of argon with about 10% of the probability of ^{36}Cl, i.e. fallout is about 2 atoms m^{-2} s^{-1}. It is also available commercially, and a promising application is as a biomedical tracer, either alone or in double-tracer experiments with ^{26}Al. Despite the comparatively short half-life of ^{32}Si, AMS offers the advantage over conventional decay counting of a smaller sample size.

AMS detection is not straightforward because of the ubiquitous nature and high isotopic abundance of the ^{32}S isobar. It is possible to achieve a high level of isobaric suppression by using the SiH$_3^-$ ion (Heinemeier *et al* 1987), but beam currents and therefore efficiencies are low. A better solution is to inject the much more intense Si$^-$ ion and to use a gas-filled magnet to separate the ^{32}Si from ^{32}S ions. This is an extremely favourable case for the application of a gas-filled magnet because $\Delta Z = 2$, and the unwanted higher-Z isobar is bent to smaller radius in the magnetic field and therefore does not contribute a low-energy tail under the ^{32}Si peak. A discrimination factor of 10^{12} can be achieved with the combination of the gas-filled magnet and a suitable detector (Popplewell *et al* 1998).

3.8.3. ^{53}Mn ($T_{\frac{1}{2}} = 3.8$ Ma) and ^{59}Ni ($T_{\frac{1}{2}} = 60$ ka).   These two isotopes are considered together because the stable ^{53}Cr and ^{59}Co isobars pose essentially identical problems and because the principal applications of both have been to meteorites. Chromium and cobalt are ubiquitous contaminants and are difficult to separate chemically from manganese and nickel. In both cases the interfering isobar is *lower* in Z and by only one unit, which makes their separation by a gas-filled magnet more difficult than is the case for ^{32}Si. Nevertheless, gas-filled magnets have been used successfully (Knie *et al* 1997, Korschinek *et al* 1994) and sensitivities of $\sim 10^{-11}$ and $\sim 10^{-13}$ in the ^{53}Mn/Mn and ^{59}Ni/Ni ratios have been achieved.

If the concentration of the isobar can be reduced chemically below 100 ppb, then it is possible to make measurements in the same way as for ^{36}Cl. To date, this approach has been applied to ^{59}Ni only. Again, higher energies are particularly advantageous, and energies of 200 and 140 MeV have been employed by Paul *et al* (1993) and Klein *et al* (1995) respectively. Sensitivities in both cases are $\sim 10^{-13}$ in the ^{59}Ni/Ni ratio and are limited by background from the relatively high (>1 kHz) counting rates of ^{59}Co.

Another approach is to fully strip to ^{53}Mn^{25+} or ^{59}Ni^{28+} ions after acceleration but before the final magnetic analysis. Korschinek *et al* (1987) used the combination of an MP tandem followed by a linear accelerator to produce 300 MeV ^{53}Mn ions. At this energy, the full-stripping probability is, however, only 0.1%. In contrast, Kutschera *et al* (1993) used the Atlas linear accelerator at Argonne National Laboratory to impart ~ 600 MeV to ^{59}Ni ions. At this energy, $\sim 25\%$ could be fully stripped by passage through a thick carbon foil. Again, the sensitivity achieved in the ^{59}Ni/Ni ratio was about 10^{-13}.

Another alternative, which is being pursued for the measurement of ^{59}Ni in nuclear waste or for biomedical applications where levels may be substantially higher than in meteorites, is to use the technique of projectile x-ray emission (section 2.2.5). McAninch *et al* (1997) have demonstrated a sensitivity of $\sim 10^{-11}$ using this technique.

3.8.4. ^{63}Ni ($T_{\frac{1}{2}} = 100$ a).   The measurement of ^{63}Ni, produced by the ^{63}Cu(n, p)^{63}Ni reaction, may provide an alternative means of establishing the fast-neutron dosimetry of the Hiroshima and Nagasaki bombs. McAninch *et al* (1997) are employing the projectile x-ray emission technique to separate it from the ^{63}Cu isobar, and report a sensitivity limit from their initial measurements which already approaches that of decay counting.

3.8.5. ^{79}Se ($T_{\frac{1}{2}}$ = 1.1 Ma). Pathologies due to both too little and too much selenium are known but the biochemistry of Se is poorly understood. Selenium-79 may, therefore, be a useful biomedical tracer. The principal challenge to its detection by AMS is its isobar, ^{79}Br. Since silver bromide is widely used as a mask for ^{36}Cl measurements (see section 3.2 above), high bromine counting rates might be anticipated from ion sources that have been used for ^{36}Cl measurements. Indeed, an initial attempt to measure ^{79}Se was thwarted by high bromine rates (McAninch *et al* 1995). Measurements at the levels required for biomedical studies will require both a reduction in the bromine contamination of the sample and ion source, as well as a detection technique, such as projectile x-ray emission or a gas-filled magnet, which can discriminate effectively between ^{79}Br and ^{79}Se.

3.8.6. ^{90}Sr ($T_{\frac{1}{2}}$ = 28.5 a). Although ^{90}Sr can be measured with high sensitivity using conventional decay counting, AMS offers the advantage of a potentially faster response in the event of a nuclear accident. Again, the principal difficulty arises from the stable isobar, ^{90}Zr, and higher energies are required in order to be able to discriminate between ^{90}Sr and ^{90}Zr. Paul *et al* (1997), using a ^{90}Sr energy of 131 MeV, have reported the best sensitivity to date, corresponding to ^{90}Sr/Sr $\sim 3 \times 10^{-13}$. Korschinek *et al* (1994) have also reported ^{90}Sr measurements using a gas-filled magnet.

4. Applications

AMS has found application in many areas of science. Within a given area, more than one isotope may be used, and some applications employ two isotopes to provide complementary information. Hence, the approach adopted here is to group applications by area rather than by isotope. The list of applications is now very extensive, and a review such as this could not possibly do justice to them all. Instead, I will concentrate on the more recent developments, particularly in those areas where growth seems likely. There are several good reviews of the application of AMS to specific areas to which the reader is referred for more detail; these will be referenced below under the appropriate topic.

4.1. Archaeology

The importance of ^{14}C to archaeology much predates the advent of AMS, of course, but the small-sample capability of AMS has opened many new possibilities. It also has an increasingly crucial role to play in establishing the integrity of a date by addressing two key issues. The first is the question of provenance; whether an object found in a particular location is truly *in situ* or was moved there by biological or physical activity. By making it possible to date individual pieces of charcoal or seeds, for example, AMS can often provide an answer. The second issue is the extent to which the carbon in an object is representative of its original carbon. Bone, for example, is prone to loss of the protein collagen which is its principal carbon-containing component, and often only a small amount of collagen is available for dating. Moreover, the rather open structures of bone or charcoal are prone to absorb organic compounds from the soil in which they are buried, which may contain carbon of more recent origin. Because AMS requires only a mg of carbon, a rigorous chemical pre-cleaning of the sample is possible. Similarly, other objects can be subjected to the separation of individual components or to a more stringent chemical pre-treatment than is in general possible for conventional decay counting.

The hope that the superior efficiency of the AMS technique would allow ^{14}C dating to be pushed back beyond the $\sim$50 000 year limit of conventional decay counting has not, however,

been realized to date, and the present AMS limit is similar to that of decay counting. To a large extent, this limit is intrinsic in the sense that the older the sample, the greater the effect of any more recent carbon acquired by the sample in the course of its subsequent history. Although samples may be put through rigorous cleaning procedures, it takes only 0.2% of modern carbon to give a very old sample an apparent age of 50 ka. In addition, traces of modern carbon may be incorporated during sample processing, and it has not so far proved possible to reduce this below ~5 μg. If incorporated into 3 mg of dead carbon, which is a typical sample size for AMS, this would correspond to an apparent age of ~50 ka.

Several examples of the application of AMS radiocarbon dating to archaeological finds are given below. These have been chosen to be illustrative, and are in no way meant to be complete.

4.1.1. Cave and rock art. The last decade has seen a sequence of increasingly spectacular finds of cave art, particularly in France where the 1991 find of the Grotte Cosquer near Marseilles was followed in 1994 by the discovery of the Grotte Chauvet in the Ardeche. Prior to the advent of AMS, dating of such finds would have been forced to rely on stylistic interpretation and association with artefacts on the cave floor. AMS, however, has allowed the ^{14}C dating of the paintings themselves via the analysis of milligram amounts of charcoal, or other organic matter incorporated in the pigments, without significant damage to the art. Following the first successful demonstration in the French cave of Cougnac (Lorblanchet *et al* 1990), this method was employed in 1992 to date stylistically similar paintings of bison in caves at Niaud in France and at Altamira and El Castillo in Spain which ranged in age between 12.9 and 14 ka (Valladas *et al* 1992). Hence the techniques were in place to permit rapid dating of the new finds at Grottes Cosquer and Chauvet. At Cosquer, two stages are evident, dating to 19 and 27 ka respectively, (Clottes *et al* 1992). Chauvet, which boasts 216 animals of remarkable stylistic sophistication, is older still at 31 ka, based on concordant dates from three separate paintings (Clottes *et al* 1995). These dates are the earliest ever obtained for prehistoric paintings. Since *homo sapiens* is known to have been present in the Middle East more than 90 ka ago, and since Grotte Chauvet indicates that sophisticated art was already being practiced 31 ka ago, these finds raise the expectation that even earlier sites may be found. If and when they are, AMS radiocarbon dating will no doubt have an important role to play. Similar techniques are being applied to rock art in the Americas and Australia in order to shed new light on the antiquity and development of human occupation of these continents.

4.1.2. The Ice Man. In September 1991, the mummified corpse of a male human body in an excellent state of preservation eroded out of a glacier in the Ötztal Alps, South Tyrol, Italy. This remarkable find included clothes and shoes, a bow, a quiver of arrows, and a hand axe (Spindler 1994). AMS has had a key role to play in the dating of this Ice Man, with the small sample capability allowing measurements on grass from his straw cape and shoes as well as on the body itself via bone and tissue specimens. Several laboratories were involved, and a concordant set of results placed the date of his death at 4546 $\pm$ 17 radiocarbon years before the present (Hedges *et al* 1992, Bonani *et al* 1994, Prinoth-Fornwagner and Niklaus 1994). Because the calibration of radiocarbon age in terms of true calendar age is rather flat in this region (see section 4.1.4), the small error on the radiocarbon age translates into a much wider range in calendar age which falls between 3100 and 3350 BC. Nevertheless, when combined with evidence from the artefacts found with the body, this is sufficiently precise to place the Ice Man in one of two cultures which existed south of the Alps around this time (Prinoth-Fornwagner and Niklaus 1994).

4.1.3. Authentication.   Gove, in a letter to the Archbishop of Turin in 1978, first proposed using the then brand new technique of AMS to date the famous Shroud of Turin. It was to be ten years, however, before measurements were finally performed by AMS laboratories at Arizona, Oxford and Zurich. Each received about 2 cm^2 of the linen from the Shroud. The final results from the three laboratories were in excellent agreement (Damon *et al* 1989), and pointed to a medieval date (1290–1360 AD at 90% confidence) for the Shroud. This date is close to the year 1353 when the Shroud entered the historical record. Gove (1996) has given a very readable account of the sequence of events which culminated in the successful dating of the Shroud.

Less controversially, the small sample capability of AMS has allowed radiocarbon dating of some of the Dead Sea Scrolls. These are a collection of ∼1200 manuscripts recovered from cave sites near the Dead Sea following the first discovery at Qumran in 1947. They are ascribed to the Essenes, one of three major religious movements of Judaism who settled the Qumran site around 100 BC and abandoned it in AD 68. A few bear the date of copying, but dating for most has relied upon paleography, the study of ancient writings. Precise radiocarbon measurements provide a means of validating the paleographic assignments. Four manuscripts which bore the date of copying were dated by AMS at Zurich (Bonani *et al* 1992), and the results were in good agreement with the known dates. Ten other manuscripts were also dated, and, with a single exception for which the AMS date was 200 years older, the paleographic and radiocarbon dates were found to agree within the uncertainties of the two methods. Measurements on additional scrolls have recently been carried out at Arizona (Jull *et al* 1995) with similar results.

A thriving mini-industry using AMS radiocarbon dating to authenticate *objets d'art* such as antique furniture, paintings and tapestries has also developed over the past few years.

4.1.4. Calibration of the radiocarbon timescale.   An archaeologist is generally interested in the age of a sample in calendar years, whereas the raw datum from a radiocarbon measurement, be it by AMS or decay counting, is the $^{14}C/^{12}C$ ratio in the sample submitted for dating. Since the original source of the carbon was atmospheric CO_2 and since the $^{14}C/^{12}C$ ratio in this source has not been constant in time but has fluctuated in response to a number of factors (section 4.4), the relationship between the measured ratio and the calendar age of the sample is not a simple one. Fortunately, there are natural archives which can be precisely dated by other means and which therefore permit a calibration of the radiocarbon timescale in terms of calendar time.

Foremost among the archives are tree rings. A continuous annual record has been established back to 12 ka before present, and the calibration curve for this period has been constructed by high-precision decay counting of decadal or bidecadal sequences of rings of known age (Stuiver *et al* 1993). A section of the calibration curve is shown in figure 10. Calibration programs are available which utilize this curve to translate a given radiocarbon age and uncertainty into the corresponding range of calendar ages.

Beyond 12 ka, one must rely on other archives such as the coral record. Corals can be independently dated by mass-spectrometric determination of the relative proportions of ^{234}U and its ^{230}Th decay product. Comparison of the U/Th and radiocarbon dates indicates that the divergence between the radiocarbon and calendar timescales continues to increase beyond the end of the tree-ring calibration (Bard *et al* 1990a, 1990b, 1992, 1993, Edwards *et al* 1993). This divergence, which is ∼1 ka at 10 ka, has increased to 2.5 ka by 15 ka. Although the coral data are sparse beyond 15 ka, the difference between the two time-scales appears to further increase to ∼3 ka at 20 ka and may be as much as 5 ka at 30 ka (Bard *et al* 1993). The more recent work has employed AMS for the radiocarbon measurements because it allows a much more rigorous cleaning of the sample than was possible for the earlier decay-counting measurements.
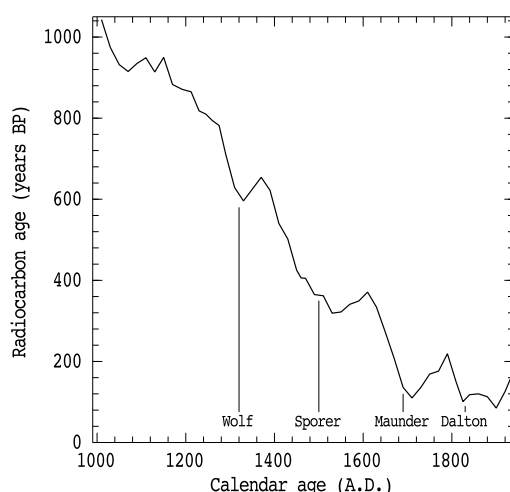
Figure 10. A portion of the ^{14}C calibration curve. Minima in this curve, which correspond to periods of elevated ^{14}C production, line up with the well-known minima in sunspot activity. (After Stuiver *et al* 1993).

Certain lakes exhibit annual sedimentary layers called varves which extend beyond the tree-ring calibration. Usually it is not possible to follow these sequences to the present day, and the principal difficulties in using them for calibration are to establish an absolute reference time somewhere in the sequence and to identify missing sections. AMS measurements on macro-fossils such as leaves, twigs or insect wings which are found in the layers provide the radiocarbon data. Studies have been carried out in Sweden, where a varve chronology has been established on the basis of hundreds of overlapping sequences (Wohlfarth *et al* 1995), and in lakes in Switzerland (Hajdas *et al* 1993), Germany (Hajdas *et al* 1995), Poland (Goslar *et al* 1995) and Japan (Kitagawa *et al* 1995). There is good agreement between the varve data and the coral data back to ~12.5 calendar ka BP, but beyond that the two appear to diverge. A more recent data set from the Japanese lake (Kitagawa and van der Plicht 1998) is, however, in much better agreement with the coral data. A good match is also obtained between the coral data and a calibration based upon a varved marine sediment core from the Caribbean (Hughen *et al* 1998).

Voelker *et al* (1998) have also produced a calibration back to 54 radiocarbon ka by ^{14}C dating foraminifera in a marine core from the Iceland sea. The absolute timescale of the core was established by correlating its δ^{18}O temperature record with that of the GISP-2 ice core from Greenland which has been dated by annual-layer counting.

Bard (1998) has recently reviewed the status of the radiocarbon calibration and its geophysical and geochemical implications.

4.2. Exposure-age dating

The long-lived isotopes ^{10}Be, ^{26}Al, and ^{36}Cl are produced *in situ* at or near the earth's surface by interactions between secondary cosmic rays and suitable target nuclei in rock. Secondary cosmic rays are fast neutrons and muons which are themselves produced by interactions in the atmosphere between energetic primary cosmic rays and atomic nuclei. Principal targets for ^{10}Be and ^{26}Al are respectively the oxygen and silicon in quartz (SiO_2), while ^{36}Cl may be produced from calcium and potassium or by the capture of slow neutrons by ^{35}Cl. Attenuation

Table 4. Production rates of cosmogenic isotopes at sea level and high latitude.

Isotope	Target	Production rate (atoms g^{-1} a^{-1})	Reference
^{10}Be	SiO$_2$	6.0	Nishiizumi *et al* (1989a)
		4.8	Clark *et al* (1995)
^{26}Al	SiO$_2$	36.8[a]	Nishiizumi *et al* (1989a)
^{36}Cl	Ca	54	Stone *et al* (1996a)
		73	Phillips *et al* (1996)
	K	154	Phillips *et al* (1996)
		175	Evans *et al* (1997)

[a] The ratio of production rates for ^{26}Al and ^{10}Be is 6.0.

lengths for fast neutrons in rock are ∼60 cm, while for the more penetrating muons they are ∼5 m. Hence, this *in situ* production is very much a near surface phenomenon. Provided that the production rates are known, the build-up of one or more of these isotopes may be used to determine the time of first exposure of the rock at the earth's surface. It is possible in this way to date such geological processes or features as glacial advance and retreat, meteorite impacts, fault movements, lava flows and landslides, and wave-cut platforms. Production rates are very low, and it has only been with the advent of AMS that measurements on terrestrial surfaces have become feasible, although the idea of cosmic-ray exposure dating may be traced back to earlier work on meteorites and on lunar samples.

Typical production rates at sea level and high latitude are shown in table 4. Cosmic-ray flux increases with altitude as attenuation by the atmosphere decreases, and is lower at the equator than at the poles because the earth's magnetic field deflects the primary cosmic rays more effectively at lower latitudes. In a seminal paper, Lal and Peters (1967) assembled the relevant information on cosmic-ray fluxes and interaction probabilities to estimate production rates as well as the scaling factors for altitude and latitude. A more recent discussion of these issues is contained in reviews of *in situ* produced cosmogenic isotopes in terrestrial rocks by Lal (1988, 1991). Theoretical calculations of production rates have also made considerable progress (Mazarik and Reedy 1995).

Because the relevant nuclear cross sections for the production of a specific isotope are not in general well known, much effort has been expended in recent years on the empirical determination of production rates using surfaces of known age (Nishiizumi *et al* 1989a, Zreda *et al* 1991, Clark *et al* 1995, Phillips *et al* 1996, Stone *et al* 1996a, Nishiizumi *et al* 1996, Evans *et al* 1997). Glacially polished surfaces or lava flows have been used, although there are sometimes difficulties in establishing reliable dates for these surfaces by independent techniques. For example, ^{10}Be and ^{26}Al production rates were first determined by Nishiizumi *et al* (1989a) on the basis of an 11 ka age for glacially polished surfaces in the Sierra Nevada. Clark *et al* (1995) have subsequently suggested that this age is at least 17% too young, and that production rates should be correspondingly lower. Additional complexity is introduced by the fact that the production rates themselves may not be constant in time due to variations in the intensity of the earth's magnetic field (Clark *et al* 1995). Consequently, production rates are probably not known to better than 10% at present. Nevertheless, this is more than adequate to address important dating issues. Further, the precision of the method should improve as knowledge of the production rates improves, since the uncertainty in the production rate generally dominates the overall uncertainty. It follows that it is important that the production rates employed in deriving quoted exposure ages should be clearly stated.

Earlier reviews of surface exposure dating may be found in Dorn and Phillips (1991) and Cerling and Craig (1994).

4.2.1. Conditions for reliable exposure-age dating.   The integrity of an exposure-age date depends upon careful sample selection in order to ensure that the following conditions are met:

 (i) Prior exposure of the surface should have been negligible. The contribution of *in situ* produced isotopes from a prior exposure can be significant if, for example, glacial scouring has removed less than a few metres of bedrock.

 (ii) The surface should have been free of snow or debris cover since exposure. Where possible, samples are taken from large boulders or sloping bedrock surfaces.

(iii) Erosion, which removes material together with its cosmogenic-isotope inventory from the surface, and exposes material from deeper down which has been exposed to fewer cosmic rays, should have been minimal. Typical erosion rates of hard rock in low-rainfall areas are in the range 1–5 mm ka^{-1}, and under these conditions at least 20–100 ka of exposure is required before erosion becomes significant. Bedrock which still bears glacial striations is unlikely to have eroded by more than a few millimeters.

(iv) For ^{10}Be and ^{26}Al produced in quartz, only a single production rate (from oxygen and silicon, respectively) need be known for each.

 (v) For ^{36}Cl the situation is more complex, and it has been necessary to determine separately the production rates from calcium, potassium and chlorine. The concentrations of these elements may vary locally, and any revision of one of the production rates may therefore have a variable effect on the exposure ages deduced from different samples. The ideal, not always achievable, is to choose the system such that one of the production mechanisms is dominant. This can be satisfied in one of three ways:

- by choice of rock type, calcite for example (Stone *et al* 1996a),
- by mineral separation, of potassium feldspar, for example (Evans *et al* 1997),
- by crushing to release the fluid inclusions in which any ^{36}Cl present must have been produced via neutron capture by ^{35}Cl (Bierman *et al* 1995).

4.2.2. Glacial advance and retreat.   Glacial chronologies can be established by exposure-age dating of moraine boulders and glacially polished bedrock, which has the advantage of dating the actual surfaces created by glacial advance or retreat. It is more generally applicable in this context than radiocarbon dating, which must rely upon sediments from lakes or bogs created behind moraines, or fragments of vegetation overrun by moraines, to provide only lower and upper limits on the age, respectively.

Several studies of North American alpine glaciations have been reported. Alpine glaciers respond more rapidly than large continental ice sheets to changes in temperature and precipitation, and hence may provide better time resolution for detecting rapid shifts in climatic conditions. Phillips *et al* (1990) and Zreda *et al* (1994) have dated sequences of moraines in the Sierra Nevada Range in California using ^{36}Cl. Ages vary between 21 and 200 ka. Another late Pleistocene moraine sequence in Wyoming has been dated by Gosse *et al* (1995a, 1995b) using ^{10}Be. These data represent the current state of the art in exposure-age dating, with 1σ errors of 3% on ^{10}Be ages (excluding the production rate uncertainty). The paleoclimatic information derived from the Wyoming studies includes the duration of the last glacial maximum (LGM) at this location and evidence that the Younger Dryas cold period, which extended from 12.8 to 11.5 ka BP in northern Europe, also occurred in North America.

Additional boundary conditions for reconstructions of climates during glacial periods may be provided by the maximum thicknesses of continental ice sheets. In this context, it

has been proposed that 'trim lines', which are observed around hill sides in formerly glaciated mountainous areas in northern Europe and Canada and which mark a sharp transition from summit regions of highly weathered bedrock to glacially scoured surfaces at lower altitude, may represent the maximum vertical extent of the ice sheets. Brook *et al* (1996) and Stone *et al* (1998b) have tested this conjecture by measuring the exposure ages of surfaces above and below trim lines on mountains in western Norway and Scotland, respectively. Their results provide strong support for the above interpretation, as well as yielding dates for the times at which these ice sheets retreated from their maximum heights.

A closely related problem is the dating of coastal rock platforms which represent still stands of effective sea level. Stone *et al* (1996b) have used exposure-age dating to show that a platform in western Scotland was cut about 10 ka ago when rising sea levels were in balance with post-glacial rebound of the land surface.

While the above studies in the northern hemisphere have, of necessity, been focused on late Pleistocene glaciations, the glaciation history of Antarctica may be extended much further back in time as a consequence of the extremely low rates of erosion (see section 4.3 below) that prevail in the hyper-arid regions where much of the exposed rock surfaces are found. The first indications from exposure-age measurements of just how low erosion rates could be in Antarctica and how long some surfaces had been exposed were reported by Nishiizumi *et al* (1991a) who measured ^{10}Be and ^{26}Al in quartz from four widely separated locations. Several of the samples were found to have exposure times of greater than 1 Ma, and almost all were eroding at less than 1 μm a^{-1}. One sample, in particular, had been exposed for more than 4 Ma with an erosion rate of less than 0.06 μm a^{-1} throughout that time. Subsequent studies with similar conclusions have been reported by Brown *et al* (1991), Ivy-Ochs *et al* (1995) and Brook *et al* (1995).

It is possible to use the accumulation of 'garden variety' ^{10}Be (see section 4.3.3 below) as a chronometer. Pavich and Vidic (1993) have dated a sequence of glacio-fluvial terraces in Slovenia by measuring the total inventory of ^{10}Be in the soils developed on the terraces, and comparing this with an assumed annual fallout of ^{10}Be to derive an age. Although the method is subject to larger uncertainties than exposure-age dating, useful information can be obtained.

4.3. Landscape evolution and catastrophic events

Landscapes erode and are modified by catastrophic events such as meteorite impacts, lava flows, landslides, and movement along fault lines. Cosmogenic isotopes are applicable to each of these processes, determining rates of erosion or the timing of the catastrophic events. Of course, glaciers, discussed in some detail above, are also powerful agents of landscape evolution. The diversity of geomorphological applications of AMS is illustrated in a paper by Nishiizumi *et al* (1993). Recent reviews of AMS in the earth sciences include Morris (1991), Finkel and Suter (1993), Cerling and Craig (1994) and Rucklidge (1995).

4.3.1. Erosion. Concentrations of *in situ* produced isotopes in rock surfaces are influenced both by the exposure age of the surface and by the rate at which it is being eroded. In different geomorphic contexts, measurements of one or more isotopes can therefore yield valuable information about either or both of these properties. Lal (1991) has discussed this cosmic-ray labelling of erosional surfaces in some detail. For a constant erosion rate, ϵ, the build-up of *in situ* produced isotopes at the surface proceeds according to:

$$N(t) = \frac{P}{(\lambda + \epsilon\rho/\mu)}(1 - e^{-(\lambda+\epsilon\rho/\mu)t})$$
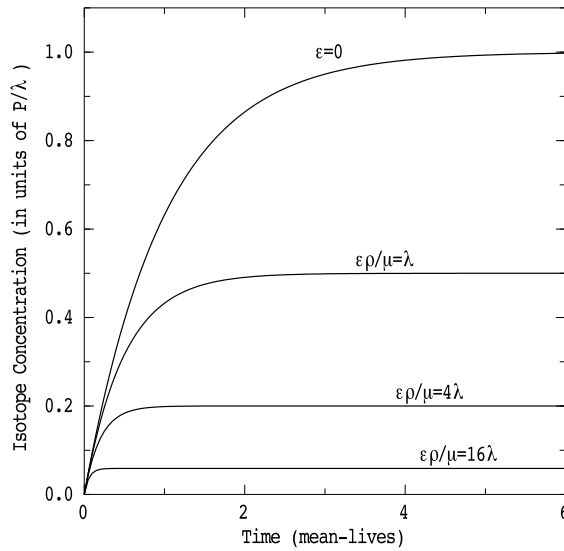
Figure 11. The surface concentration of a cosmogenic isotope in rock as a function of time and for different erosion rates. For ^{36}Cl, one mean life is 430 ka, and P/λ at sea level and high latitude is 1.3×10^7 atoms g^{-1}.

where P is the production rate in atoms g^{-1} a^{-1}, λ is the decay constant of the isotope in a^{-1}, μ is the attenuation length of the cosmic rays in rock. A value of 160 g cm^{-2} is widely used. ρ is the density of the rock.

This is illustrated in figure 11. Note that the curves approach saturation with a characteristic time of $1/(\lambda + \epsilon\rho/\mu)$. If the surface has been exposed for a time which is long compared to this characteristic time, then saturation will have been reached and the erosion rate can be determined directly from the measured concentration, N, of the cosmogenic isotope via the simple expression:

$$\epsilon\rho/\mu = \frac{P}{N} - \lambda.$$

The above expressions strictly apply only when the depth dependence of production is described by a simple exponential with characteristic length μ. This is satisfied if spallation is the only significant mechanism of cosmogenic isotope production, but production by muon and neutron capture leads to departures from a single exponential form. Cosmic ray muons are much more penetrating than the fast neutrons responsible for spallation, and although muon capture contributes only between 1 and 10% of the production of ^{10}Be, ^{26}Al or ^{36}Cl at the surface (Stone *et al* 1996a, 1998, Brown *et al* 1995a, Nishiizumi *et al* 1994, Strack *et al* 1994), its fractional contribution increases with depth and exceeds that of spallation below $\sim$2 m. Hence, on a rapidly eroding surface, a substantial fraction of the cosmogenic-isotope inventory at the present-day surface will have been produced by muons at depth, and it is essential to take muon production into account when estimating erosion rates. For a calcite surface eroding at 30 μm a^{-1}, for example, neglect of the muon contribution leads to a 30% underestimate of the erosion rate (Stone *et al* 1998a). In contrast, the production of ^{36}Cl by neutron capture on ^{35}Cl has a depth dependence which peaks about 20 cm below the surface due to diffusive loss of slow neutrons at the rock–air boundary (Dep *et al* 1994a, Liu *et al* 1994). It is possible to turn these different depth dependences to advantage because a depth profile contains more information on the exposure and erosion history than a single surface measurement. Stone

et al (1998a) have explored possibilities arising from the contrast between muon and spallation production, while Dep *et al* (1994b) and Zreda *et al* (1994) have exploited the different depth dependence of spallation- and neutron-produced ^{36}Cl to derive both exposure ages and erosion rates.

It should be emphasized that the cosmogenic-isotope method measures erosion over a timescale determined by the characteristic time, $1/(\lambda + \epsilon\rho/\mu)$. This is 300 ka for an erosion rate of 1 μm a^{-1}, reducing to 60 ka at 10 μm a^{-1}. Other tools used by the geomorphologist, such as fission tracks or micro-erosion meters, probe the erosion rate over much longer and much shorter timescales respectively, and are not necessarily measuring the same quantity as the cosmogenic isotopes. Note also that a constant rate of erosion is assumed, whereas in reality erosion on a local scale is often discontinuous with sheets of material spalling off due to freeze–thaw conditions or the action of fire (Bierman and Gillespie 1991). Provided, however, that the characteristic depth of the spalled fragments is small compared to the attenuation length in the rock of the isotope-producing cosmic radiation, such discrete events do not lead to serious departures from an average erosion rate.

Stone *et al* (1994) have measured surface concentrations of ^{36}Cl to estimate erosion rates of limestone features across a wide range of climatic regimes in Australia and Papua New Guinea. They find values that range from <4 μm a^{-1} in arid central Australia to nearly 200 μm a^{-1} in the New Guinea highlands. Bierman and Turner (1995) have demonstrated, using ^{26}Al and ^{10}Be, that erosion rates of a number of South Australian inselbergs (granitic domes) are as low as 0.6 μm a^{-1}.

4.3.2. Complex exposure histories. If an eroding surface has not reached saturation, or has undergone burial and re-exposure, then a surface measurement of a single isotope is insufficient to determine the erosion rate, exposure age, or history of the surface. One solution, noted above, is to measure a depth profile of a single isotope. Another is to measure the concentrations of two isotopes of different half-lives. Extensive use has been made of the ^{26}Al–^{10}Be pair extracted from the same quartz sample. A plot of ^{26}Al/^{10}Be ratio versus ^{10}Be concentration as shown in figure 12, which was introduced by Nishiizumi *et al* (1991a), facilitates an intuitive visual interpretation of the results. With increasing exposure time, the ^{26}Al/^{10}Be ratio drops from its production value of 6.0 and, in the absence of erosion, follows the upper solid curve, finally attaining a saturation value of 2.8. An eroding surface follows a different trajectory on the plot, reaching saturation with a higher value of the ^{26}Al/^{10}Be ratio. A series of trajectories corresponding to different erosion rates are shown on the figure. The locus of the end points of all such trajectories is the lower solid line. A continuously exposed surface must lie on or between the upper and lower lines. In this case, both the erosion rate and exposure time can be determined from measurements of the concentrations of the two isotopes. Because the half-lives of this particular pair of isotopes differ by only a factor of two, however, high precision in the measurement of both the ^{10}Be and ^{26}Al concentrations is required if meaningful conclusions are to be obtained. If, on the other hand, the surface has not been exposed continuously, but has undergone burial followed by re-exposure, more ^{26}Al than ^{10}Be will have been lost by decay during the period of burial, and the data point may lie below the lower curve. Although such a point is sure evidence for an extended period of burial, it does not determine the precise history of burial and re-exposure because the route to a particular point is not unique. The route is unique, however, for a sample that has remained buried after a prior exposure, and Granger *et al* (1997) have exploited the change in ^{26}Al/^{10}Be ratio caused by extended burial to date the emplacement of river sediments in caves.

Brown *et al* (1994), in another variation on this theme, have demonstrated that an iron-crust surface in Burkina-Faso is accumulating by showing that quartz pebbles under the surface
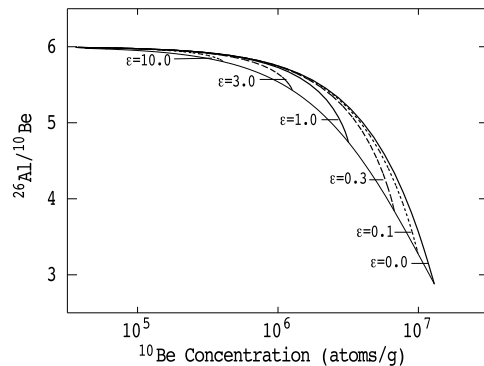
Figure 12. Plot of ^{26}Al/^{10}Be ratio versus ^{10}Be concentration for quartz exposed at the earth's surface. The upper solid curve is for zero erosion, and a series of curves for progressively higher rates of erosion (in mm ka^{-1}) are also shown. The lower solid curve is the locus of the end points of all such curves.

have higher concentrations of ^{26}Al and ^{10}Be than on the surface. This is the signature of a surface undergoing slow burial, since a pebble which originally had the erosion-determined surface-saturation value can accumulate additional isotope if it is removed from the erosive environment while still being exposed to cosmic rays.

Brown *et al* (1995b), Bierman and Steig (1996) and Granger *et al* (1996) have explored the feasibility of estimating average basin-wide denudation rates by a simple measurement of *in situ* produced ^{10}Be in sediment carried out of the basin. Provided that the quartz content of the bedrock in the basin is reasonably uniform and sediment storage within the basin is minor, it is possible to determine the average denudation rate with an uncertainty of $\sim$35%, at least for small catchments.

A related application is the dating of lake and stream terraces via *in situ* produced ^{10}Be in quartz cobbles. Studies in western China and California have been reported by Molnar *et al* (1994) and Trull *et al* (1995), respectively.

4.3.3. Soil development and erosion. Many landscape surfaces are not bare rock but have soils developed on them. Soil loss is a form of erosion, and soil is also continually created by weathering of the underlying bedrock. In addition, soils may accumulate due to transport by water or wind from elsewhere. Both 'garden variety' ^{10}Be and *in situ* produced ^{10}Be and ^{26}Al have been employed in studies of the rates of these processes.

'Garden variety' ^{10}Be is produced in the atmosphere by cosmic ray spallation of nitrogen and oxygen nuclei, attaches to aerosols and falls out in rainfall. The fallout rate appears to be well-correlated with precipitation, and several measurements indicate that it is about 1.5×10^4 atoms cm^{-3} (Monaghan *et al* 1986, Brown *et al* 1989). After fallout, it attaches to soil particles and follows their subsequent history, provided that the characteristic time for loss of ^{10}Be in solution is long compared to the soil residence time. Laboratory measurements under various conditions of pH and mineralogy have been performed by You *et al* (1989) using ^{7}Be as tracer. They found that, under neutral conditions, most mud, silt and clay minerals have retention times of about 500 000 years. Field studies of the retention of ^{10}Be have been reported by Monaghan *et al* (1983) and Pavich *et al* (1986) for soils in temperate regions of North America. Residence times in the top metre of the soil were found to range between 20 000 and 500 000 years, with clay-rich soils being the most retentive.

Knowledge of the rates of bedrock-to-soil conversion, and of soil loss due to anthropogenic
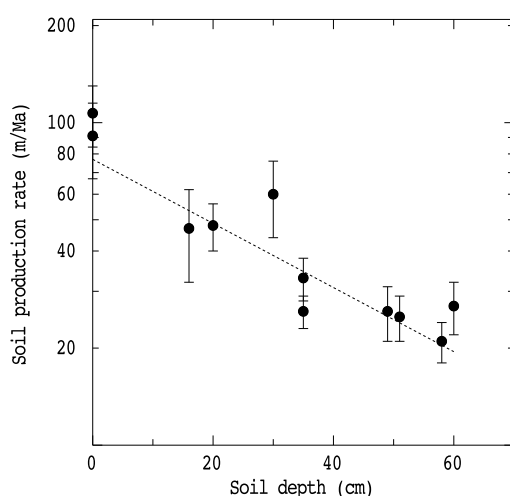
Figure 13. Soil production rates (calculated from *in situ* produced cosmogenic [10]Be and [26]Al in bedrock samples) versus soil depth for a series of sites in Tennessee Valley, Marin County, California (after Heimsath *et al* 1997).

influences, is required if the sustainability of modern agriculture and pastoral activity is to be evaluated. Cosmogenic-isotope studies have made contributions in this area. Monaghan *et al* (1992, 1994) have estimated bedrock-to-soil conversion and soil-loss rates on a hill slope in California by measuring the inventory of 'garden variety' [10]Be in the soil. Heimsath *et al* (1997) have used [10]Be and [26]Al, produced *in situ* in the bedrock underlying the soil, to address the closely related problem of the correlation between soil depth and the rate at which bedrock is converted to soil. As shown in figure 13, bedrock-to-soil conversion rates were found to be inversely proportional to soil thickness.

Erosion and sedimentation rates have also been determined from the concentrations of 'garden variety' [10]Be in sediments. Valette-Silver *et al* (1986) measured [10]Be concentrations in sediments from Chesapeake Bay in the eastern USA to show that the introduction of European farming techniques triggered the erosion, transport and sedimentation of large quantities of [10]Be-rich, and hence topsoil-derived, soils. In a broader study of 48 drainage basins in the eastern USA, Brown *et al* (1988) measured [10]Be in sediments from a variety of locations. By comparing the [10]Be being transported from the basin with that incident upon it they were able to show that there was a net loss of soil in the upper catchments which was being stored in the coastal plain.

'Garden-variety' [10]Be has also been used to study the beryllium isotope geochemistry in tropical river basins (Brown *et al* 1992). A further application to the determination of loess deposition rates and climates in China over the past 750 ka has been reported by Shen *et al* (1992) and Beer *et al* (1993).

4.3.4. Catastrophic events. Meteor Crater in Arizona is the largest known impact crater on the Earth with an associated meteorite (Canyon Diablo), but has proved difficult to date by conventional means. Two independent exposure-age measurements have been reported by Phillips *et al* (1991) and Nishiizumi *et al* (1991b) using respectively [36]Cl and [10]Be–[26]Al produced *in situ* in large blocks of ejected material on the crater rim. There is excellent agreement between the two methods where the same block was sampled, and the oldest ages,

which are represented by several blocks in each study, all cluster around 49 ka. Strictly speaking, this is a minimum age for the crater because it neglects erosion, initial debris cover and subsequent snow cover, but the authors argue that the effect of these is likely to be minor.

Young lava flows are difficult to date by the more conventional K–Ar or Ar–Ar techniques due to problems with inherited ^{40}Ar and the long half-life (1.28×10^9 a) of ^{40}K, whereas the age range from 10–100 ka is readily accessible to the exposure-age technique. Zreda *et al* (1993) have dated the Lathrop Wells basaltic cinder cone and its associated lava flows to 81 ± 8 ka using *in situ* ^{36}Cl extracted from the whole rock. The age of this eruption is especially significant because of the site's proximity to the proposed radioactive waste repository at Yucca Mountain, Nevada.

Earthquake recurrence intervals along the Owens Valley fault in California have been estimated (Bierman *et al* 1995) from the exposure ages of boulders on debris flow fans which have been offset by earthquakes. Zreda and Noller (1998) have dated multiple prehistoric earthquakes along a fault in Montana by measuring ^{36}Cl produced *in situ* in the bedrock scarp created by movement of the fault.

Exposure dating is also well suited to landslides, allowing evaluation of the possible causes and triggers of these features, particularly in post-glacial landscapes, which has been hindered until now by a lack of reliable dating. A pilot study on a large rockslide on the Isle of Skye, Scotland has been reported by Ballantyne *et al* (1998).

4.4. Ice cores

Polar ice preserves a continuous record of atmospherically produced ^{10}Be and ^{36}Cl. Since ice cores can be dated by a number of techniques, including the counting of annual layers, the production rate and climatic factors that control the deposition of these isotopes in snow can be studied on scales from seasonal to millennial.

Production is controlled by three parameters, namely:

 (i) primary cosmic-ray intensity
 (ii) modulation of the cosmic-ray flux by changes in the solar magnetic field
(iii) geomagnetic modulation of the cosmic-ray flux.

Variations in these parameters have different characteristic timescales. It is possible in principle, therefore, to deconvolve their individual contributions to the cosmogenic-isotope record. In addition, useful paleoclimatic information may be derived from these cosmogenic-isotope archives both because deposition is influenced by climate, and because solar activity (which influences production) and solar radiance (which influences climate) are correlated.

4.4.1. ^{10}Be in ice.

Measurements of ^{10}Be in ice were pioneered by the Orsay group (Raisbeck *et al* 1981). Subsequently, groups using the facilities at Zurich and Livermore have also become involved. Several cores from both the Arctic and Antarctic have been studied, and measurements are well underway on the 3 km long GRIP (European) and GISP2 (American) cores from the Greenland summit.

Dye-3 in Greenland and Taylor Dome in Antarctica are high-accumulation sites for which annual resolution is readily achievable. Beryllium-10 concentrations have been measured in the Dye-3 core from the present back to 1400 AD by Beer *et al* (1990, 1994a), and for the past 75 years in the Taylor Dome core by Steig *et al* (1996). The 11-year Schwabe solar cycle is clearly visible in these data with an amplitude of $\sim \pm 20\%$ about the mean value, even though large short-term fluctuations due to local deposition processes are present. Longer term variations which correlate well with solar activity and with the ^{14}C tree-ring record are

also evident (Beer *et al* 1994b, Bard *et al* 1997, Bard 1998). These observations imply that the ^{10}Be concentrations in ice cores do reflect changes in production rates due to solar activity.

Ice-core evidence for geomagnetic modulation of production rates is less well established. Mazaud *et al* (1994) have compared the ^{10}Be record in the Vostok core with the record of geomagnetic field intensity and argue that the two are strongly correlated. In particular, two prominent peaks in ^{10}Be concentration at *ca.* 35 and 60 ka fall close to pronounced minima in the geomagnetic field intensity. These peaks were first observed in the Vostok and Dome C Antarctic records by Raisbeck *et al* (1987) and the 35 ka peak has subsequently been noted in other ice cores from both the Arctic and Antarctic (Beer *et al* 1992, Yiou *et al* 1997), and possibly also in marine cores (Cini Castagnoli *et al* 1995, McHargue *et al* 1995, Aldahan and Possnert 1998). There is a difficulty, however, in interpreting these peaks in terms of a reduction in the geomagnetic field. Geomagnetic shielding is ineffective near the poles, and hence a considerable fraction ($\sim$75%) of the ^{10}Be must have been produced north of 60° S and transported to Antarctica before deposition.

Whatever the origin of the peak at $\sim$35 ka, its global occurrence is proving to be a useful time marker to permit the reliable correlation of climate records between northern and southern hemisphere ice cores and other archives. The difficulties of trying to correlate these records using absolute chronologies obtained by other means is highlighted by the dates assigned to this peak in various studies, with values ranging from 32 ka (McHargue *et al* 1995) to 42 ka (Yiou *et al* 1997).

Solar and geomagnetic modulation of production rates are reflected most directly in the *flux* (in atoms cm^{-2} a^{-1}) of ^{10}Be. Climatic effects, on the other hand, would be expected to be manifested in its *concentration* (in atoms g^{-1} ice) since this is affected by precipitation. Indeed, as illustrated by figure 14, the concentration of ^{10}Be is a factor of two lower during the last 10 ka than during the glacial period which preceded it, reflecting the much higher ice-accumulation rates during the Holocene. The extent of fractionation of the oxygen isotopes is another climate proxy, and there is a good correlation between ^{10}Be concentration and δ^{18}O in cores where both have been measured (Raisbeck *et al* 1981, 1992, Yiou *et al* 1997, Finkel and Nishiizumi 1997). This correlation is clearly apparent in the GISP2 data shown in figure 14.

4.4.2. ^{36}Cl in ice. Chlorine-36 fallout is an order of magnitude less than ^{10}Be, and measurements of ^{36}Cl in ice cores are not as extensive as those of ^{10}Be. Although some measurements were performed on earlier Greenland cores (Elmore *et al* 1987, Synal *et al* 1994), the first comprehensive studies of ^{36}Cl in ice cores are being undertaken at the Zurich and Livermore laboratories on the GRIP and GISP2 cores. First results from the GRIP core have been published by Baumgartner *et al* (1997b, 1998), and show a clear correlation between ^{36}Cl concentration and δ^{18}O, similar to that observed for ^{10}Be, indicating that climate plays an important role in the deposition of this isotope as well. The *ca.* 35 ka peak also appears very conspicuously in these ^{36}Cl data as shown in figure 15, and is again attributed (Baumgartner *et al* 1998) to geomagnetic modulation of production, but in contrast to ^{10}Be in the Antarctic, requires transport of only 30% of the deposited ^{36}Cl from lower latitudes.

It has been proposed that the ratio of ^{36}Cl to ^{10}Be might be a suitable chronometer for dating old ice, on the basis that the production mechanisms and atmospheric residence times of the two isotopes are similar. This ratio has been measured in the Camp Century and GRIP cores (Elmore *et al* 1987, Yiou *et al* 1997), but unfortunately shows fluctuations of similar magnitude to those exhibited by the isotopes separately. It is likely that these fluctuations are due to differences in the mechanisms which control the deposition of the two isotopes. ^{10}Be attaches to aerosols which are washed out by precipitation, whereas ^{36}Cl is probably present in the atmosphere in gaseous form and its fallout is only weakly dependent on precipitation.
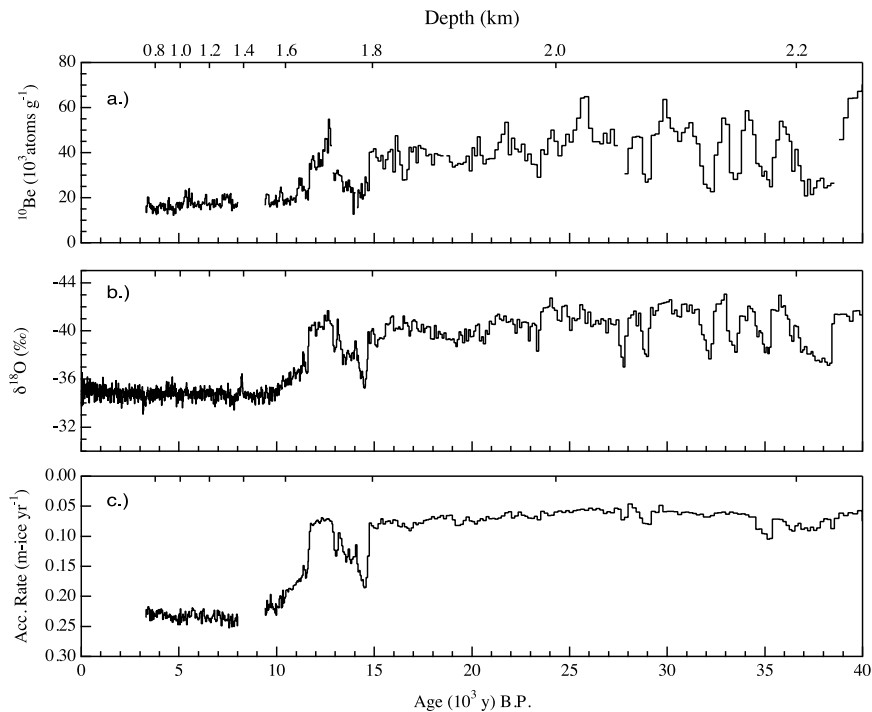
Figure 14. (*a*) The [10]Be concentration in the Greenland Ice Sheet Project 2 (GISP2) ice core (Finkel and Nishiizumi 1997). (*b*) $\delta^{18}O$ in the GISP2 core (Grootes *et al* 1993). (*c*) Ice accumulation rate (Cuffey and Clow 1997). The bottom axis indicates the GISP2 timescale and the top axis is in terms of depth. The scales for $\delta^{18}O$ and accumulation rate have been inverted for ease of comparison with [10]Be. (From Finkel and Nishiizumi 1997.)

An additional complication is that there is continental dust in the cores, and results from the GRIP core (Baumgartner *et al* 1997, Yiou *et al* 1997) indicate that there can be differences of up to a factor of two in the inventory of [10]Be depending on whether or not this dust component is included.

Not only are ice cores ideal repositories of cosmogenic fallout, but they are also unique archives of anthropogenic [36]Cl. Nuclear weapons testing, particularly in the late 1950s when high-yield tests were carried out on barges moored in atoll lagoons, injected large quantities of [36]Cl into the stratosphere where it was well mixed before falling out. Ice cores from high-accumulation sites such as Dye 3 in Greenland preserve an annual record of this fallout, which at its peak was three orders of magnitude above the normal cosmogenic rate (Elmore *et al* 1982, Suter *et al* 1987, Synal *et al* 1990). Figure 16 shows the data of Synal *et al* together with the results of a box-model analysis which provides a good description of the measured fallout if the average residence time in the stratosphere is about two years.

4.4.3. Radiocarbon measurements on air trapped in ice. The air trapped in bubbles in ice is a valuable source of information on concentrations of CO_2 and other gases in paleoatmospheres (Etheridge *et al* 1996). Since diffusion of air in and out of the ice continues until the ice reaches a depth of $\sim$80 m, the trapped air is, however, younger than the ice which encloses it. By exploiting the 'bomb-pulse' of ^{14}C at a high-accumulation site in Antarctica, Levchenko *et al* (1996, 1997) have shown that at this site where 80 m of ice accumulates in about 50 years, the
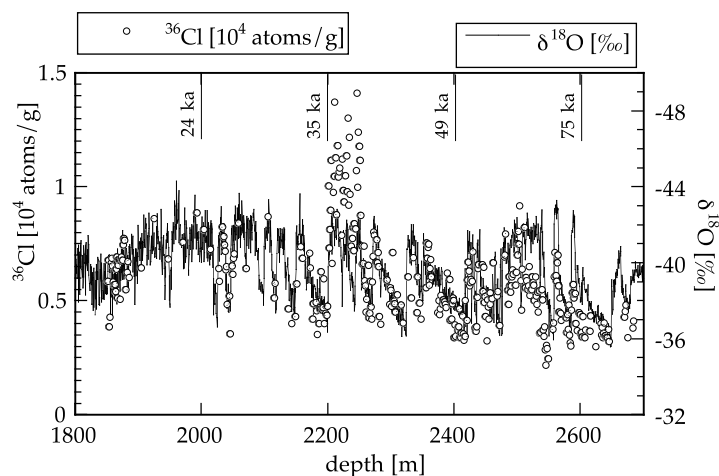
Figure 15. Chlorine-36 (circles) and $\delta^{18}O$ (solid trace) from 1800 to 2700 m in the GRIP ice core from Summit, Greenland. The $\delta^{18}O$ data and the provisional timescale are from Dansgaard *et al* (1993). (From Baumgartner *et al* 1997a.)
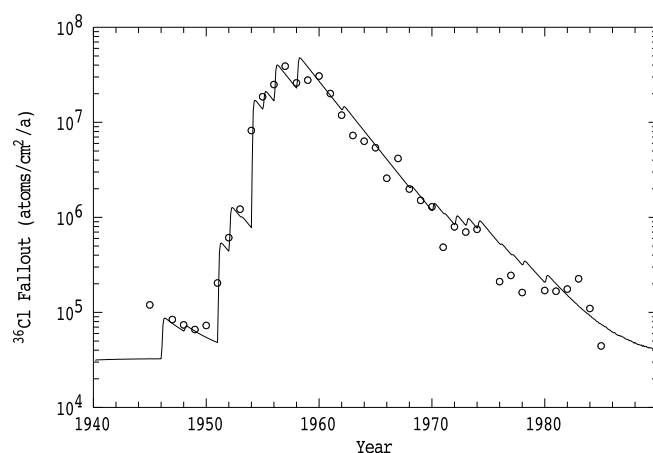
Figure 16. The ^{36}Cl bomb pulse in an ice core from Dye 3, Greenland. The solid line is the result of a box-model calculation (after Synal *et al* 1990).

air is about 40 years younger than the ice with a spread in age of only 12 years. It follows that such a site preserves a high-resolution record of air from the past few millenia.

The ^{14}C in the trapped CO_2 can also be used to date ice where annual layer counting is not possible. *In situ* production of additional ^{14}C by cosmic-ray bombardment of the ice at both the deposition and ablation sites is a complication, but can be taken into account by measuring separately the ^{14}CO and $^{14}CO_2$. Approximately equal amounts of these two species are produced by the spallation process, whereas the atmospheric component is almost exclusively $^{14}CO_2$. Van Roijen *et al* (1994) have successfully applied this method to date ice at an ablation zone in East Antarctica.

4.5. Deep-sea cores

The extent of fractionation of the oxygen isotopes by marine foraminifera is a sensitive indicator of ocean temperature. Measurements of $\delta^{18}O$ in foraminiferal shells extracted from deep-sea cores show pronounced fluctuations over the past 2.5 Ma, and this period has been conveniently subdivided into a series of 'oxygen-isotope stages' representing different climatic regimes. Establishing an absolute chronology for these stages has, however, proved to be difficult. Fortunately, the most recent part of the record, which embraces the abrupt end about 15 ka ago of the last major glaciation, and the brief return of cold conditions about 11 ka ago during the Younger Dryas period, falls within the range of radiocarbon dating. AMS, because it permits the dating of individual species of foraminifera hand-picked from cores, has been instrumental in the construction of accurate chronologies spanning these changes (Duplessey *et al* 1986, Bard *et al* 1987, Broecker *et al* 1988, Hughen *et al* 1998).

Beryllium-10 has also been measured in deep-sea cores. Contrary to expectation, observed ^{10}Be fluxes into open-ocean sediment cores are found to be a factor of two to three lower than the global average production rate (Henken-Mellies *et al* 1990), whereas in areas of high particle flux the ^{10}Be flux is enhanced by a similar factor (Wang *et al* 1996). It appears that the 500–1000 year residence time of ^{10}Be in the ocean is sufficiently long to allow preferential scavenging of ^{10}Be at areas of high particle flux. As in ice cores, evidence from marine cores for a geomagnetic influence on ^{10}Be production is equivocal. Although increases of the ^{10}Be/^{9}Be ratio are observed (Henken-Mellies *et al* 1990) near the Brunhes–Matuyama and Matuyama–Gauss magnetic reversals, increases of similar magnitude are also observed elsewhere in the core. Robinson *et al* (1995), McHargue *et al* (1995) and Aldahan and Possnert (1998) report significant anti-correlations between the ^{10}Be/^{9}Be ratio and the paleomagnetic intensity in cores from the Atlantic Ocean, Gulf of California and Caribbean, respectively.

4.6. Island-arc volcanism

Marine sediments are rich in ^{10}Be. By measuring the concentrations of ^{10}Be in lavas from island-arc volcanoes which occur along active subduction zones, it is possible to study the extent to which sediment is incorporated into subducting plates and the timescale from subduction to eruption. Ratios of ^{10}Be/Be have been measured in recent lavas from many island-arc areas (Brown *et al* 1982, Tera *et al* 1986, Monaghan *et al* 1988, Morris and Tera 1989, Morris *et al* 1990, 1993), and some are indeed characterised by high ^{10}Be/Be ratios. You *et al* (1994) have performed ^{10}Be analyses in subduction-zone sediment in order to study the mechanism of its incorporation into the subducting plate.

4.7. Oceanography

Measurements of ^{14}C in ocean water have been widely used to address questions such as the turnover and mean residence times of deep ocean water, mixing between basins, and the transfer of heat from low to high latitudes. Bomb-produced ^{14}C has played a valuable role in these studies. It is readily detectable in the upper water column, and may be used to study surface ocean circulation and atmosphere–ocean exchange processes. The amplitude of the signal is more than 20% and a precision between 0.7 and 1% is sufficient for meaningful results. The bomb pulse has not yet penetrated into the deep basins of the world's oceans, however, and lateral gradients there are due to mixing of waters which were last exposed to atmospheric exchange at different times. Gradients are typically only 2–3% across an entire basin and 0.3–0.4% precision is required. Such precision has traditionally been the preserve of decay counting, but the very large number of samples generated by the World Ocean Circulation

Experiment (WOCE) has led to the establishment of the National Ocean Sciences AMS facility at the Woods Hole Oceanographic Institute with a brief to achieve this level of precision for upward of 3000 samples per year (Jones *et al* 1990). The major attraction of AMS is that it makes possible a reduction in sample size by three orders of magnitude compared with decay counting. A 0.5 l water sample is all that is now required compared with 200 l previously, which greatly simplifies sample collection and storage. In its first five years of operation, the Woods Hole laboratory has performed $\sim$6000 measurements, of which 70% have been in the framework of WOCE, and as of mid-1996, throughput had reached $\sim$3000 samples per year at 0.35% precision (von Reden *et al* 1997). Results for surface waters from the Pacific Ocean are presented in the same paper. Other AMS oceanographic measurements of ^{14}C have been reported by Schlosser *et al* (1997) who combine new and previous data to obtain the first trans-Arctic section, and by Gislefoss *et al* (1994) as part of a program concerned with CO_2 uptake in the Nordic Seas.

Knowledge of present-day circulation in the Arctic Ocean is crucial to understanding oceanic heat transfer from low to high latitudes. Serendipitously, nuclear fuel reprocessing plants at Sellafield in Cumbria (UK) and La Hague on the Cherbourg Peninsula (France) have been potent point sources of ^{129}I since 1954 and 1970, respectively. Currents running through the English Channel and up the west coast of the UK have carried this isotope into the Arctic Ocean. Surveys of ^{129}I levels, both in surface waters over an extended area and as a function of depth, are providing valuable insights into circulation patterns and vertical mixing in this important area (Yiou *et al* 1994).

4.8. Global climate change

Methane is a potent greenhouse gas whose concentration in the atmosphere has increased dramatically over the past 50 years. Since its atmospheric lifetime is $\sim$1 year, this growth reflects ever-growing input rather than accumulation. Possible sources are natural gas (which is 'dead' in ^{14}C) from leaks in pipelines, as well as domesticated animals, landfills, biomass burning, and releases from natural systems such as the tundra as a result of global warming, all of which contain modern levels of ^{14}C. Because methane concentrations in modern air are only 1.75 ppm, AMS measurements of ^{14}C offer the very considerable advantage of requiring relatively small air samples, typically 1 m^3. Measurements of $^{14}CH_4$ from a clean southern-air sampling site in New Zealand (Lowe *et al* 1987, 1988) showed that about 25% of atmospheric methane may be fossil in origin. Similar conclusions were reached by later studies in the northern hemisphere (Wahlen *et al* 1989). Nuclear installations also emit $^{14}CH_4$, and Eisma *et al* (1994) performed measurements on methane collected in the Netherlands and correlated them with the direction of air trajectories, in order to study the regional influence of these anthropogenic sources.

The hydroxyl radical, OH, is the chief oxidizing agent in the atmosphere, but it cannot be measured directly with the accuracy required by global models of atmospheric chemistry. Its abundance can, however, be inferred from the concentration of ^{14}CO because oxidation of CO to CO_2 is driven by hydroxyl radicals with a time constant of about a month, and because the majority of ^{14}CO in the atmosphere is freshly produced by the immediate oxidation of ^{14}C produced by cosmic radiation. Brenninkmeijer *et al* (1992) have measured the ^{14}CO concentrations of clean southern hemispheric air using AMS, and conclude that there is a marked asymmetry in OH abundance between the two hemispheres. Subsequent work by Mak *et al* (1992) seems to point to significantly higher OH levels in the troposphere than had previously been assumed.

4.9. Pollution

4.9.1. Urban air pollution.   Urban air pollution is a complex mix of organic molecules which are emitted by vehicle exhausts, by fossil-fuel and biomass burning, and by industrial processes. Its remediation requires knowledge of the contributions from the different sources. Currie *et al* (1994) have used the ^{14}C content of carbon monoxide and aerosols to apportion the origins of pollution in several US cities. In a more recent paper (Currie *et al* 1997), this work has been extended to individual compounds, and in particular to polycyclic aromatic hydrocarbons (PAH), some of which are known to be highly mutagenic.

4.9.2. Discharges from nuclear plants.   Beasley *et al* (1992, 1993) have measured ^{36}Cl in groundwater and streams on and near nuclear fuel reprocessing facilities in the US, and have demonstrated that environmental releases of ^{36}Cl occur during nuclear fuel dissolution. Releases to the atmosphere are due to the escape of gaseous chlorine compounds which are formed when the fuel elements are dissolved in hot nitric acid. Direct releases to groundwater may occur as the result of effluent leakage or by past injections of low-level waste into deep aquifers. The radiological significance of these releases is negligible, but the very high sensitivity of AMS has created the opportunity for future monitoring of the movement and dispersion of contaminated water away from these facilities. A similar study of ^{36}Cl levels near the Chalk River site in Canada has been reported by Milton *et al* (1994a). AMS detection of ^{129}I may be used in a similar way (Rucklidge *et al* 1994, Rao and Fehn 1997).

AMS is also playing a role in the ongoing evaluation of the magnitude and spatial distribution of fallout from the Chernobyl accident through studies of the long-lived fission product ^{129}I (Straume *et al* 1998). Although ^{129}I itself poses no risk, the short-lived (eight days) ^{131}I constituted one of the principal health hazards of the releases from the accident, particularly to young children, because iodine is concentrated in the thyroid. Dosimetry immediately following the accident was not, however, adequate to determine its distribution and magnitude. Iodine-129 fallout is probably a much better proxy for ^{131}I than the more extensively measured ^{137}Cs because fallout of the latter occurs chiefly as particulates whereas iodine may also be present in gaseous form. Substantial enhancements of ^{129}I in rainfall at Munich and in Israel shortly after the accident were reported by Paul *et al* (1987a) and Kutschera *et al* (1988).

The nuclear-fuel reprocessing plants at La Hague and Sellafield have been prolific sources of long-lived radioisotopes to the environment, including an estimated 1.2 tonnes of ^{129}I (Yiou *et al* 1994). In addition, the Sellafield plant has released $\sim$250 kg of ^{239}Pu and lesser quantities of other long-lived actinides including ^{240}Pu and ^{237}Np. Alpha-particle counting has been the traditional method of monitoring actinides in the environment, but the sensitivity of this technique ($\sim$10^8 atoms) is not sufficient to monitor levels in humans. Fifield *et al* (1996, 1997) have shown that AMS has the requisite sensitivity (fewer than 10^6 atoms) to permit human monitoring and also to follow the dispersal of these radionuclides at greater distances from their sources.

Strontium-90 is a high-abundance fission product, which, because it is stored in the bones, is a potentially serious health hazard. In the event of a nuclear accident, a rapid assessment of the risks to the population due to this isotope is therefore important. Current radiochemical methods, which depend on the ingrowth of ^{90}Y (2.7 days), require up to two weeks. In principle, AMS can offer a response time of about two days (see section 3.8 above), and Paul *et al* (1997a) have demonstrated AMS detection of ^{90}Sr with a sensitivity at least as good as the decay-counting technique.

4.10. Biomedicine

Carbon-14 is very widely used as a tracer in biomedical research and in drug testing. AMS offers the major advantage of very much smaller doses than are required by traditional liquid-scintillation counting, thereby reducing the expense of preparing suitable amounts of labelled compounds, greatly reducing the problems of disposal, and allowing studies in humans. In addition to ^{14}C, there are other tracer isotopes including ^{26}Al, ^{41}Ca and ^{32}Si for which AMS offers advantages over decay counting.

Biological systems exhibit considerable natural variability, and meaningful conclusions can only be drawn from studies which incorporate large numbers of subjects and controls. If AMS is to play an important role in the biomedical arena, then this reality must be recognised, and emphasis placed on the simplification and automation of sample preparation and of high-throughput low-cost AMS operation.

4.10.1. ^{14}C. Most of the AMS development for biomedical applications of ^{14}C has been carried out at the Lawrence Livermore laboratory by Vogel and his co-workers. Their work is imbedded in, and draws on, a long tradition of intensive use of a very wide range of ^{14}C-labelled compounds in biomedical and pharmacological research which has traditionally been supported by liquid-scintillation counting. The very high sensitivity of AMS offers some powerful advantages to such studies, including the ability to use biologically active molecules which are selectively labelled at a single site, to study the effects of mutagens at naturally occurring levels, and to make measurements on a wider range of organs or chemical species. Much of the published work to date has been directed towards measuring, at environmentally realistic doses, the rates at which known mutagens bind to DNA. This is a vast field with its own extensive literature, and a review such as this could not hope to do justice to it. The interested reader is referred to the review articles by Felton *et al* (1990), Vogel *et al* (1990), Vogel and Turteltaub (1994) and Freeman and Vogel (1995) for discussion of these and other applications and references to the specialist literature. The particular requirements that biomedical applications impose on the AMS methodology do, however, merit some discussion.

Most importantly, high throughput is required. A typical biomedical experiment can generate hundreds of samples, and both sample preparation and AMS measurement must be geared to such numbers. Fortunately, because ^{14}C levels are high, the AMS measurements need take at most only a few minutes per sample. At present, samples are still prepared as graphite using a batch process that permits the preparation of 150–250 samples per week (Vogel and Turteltaub 1994), but there are obvious advantages in employing a gas source which uses CO_2 directly.

In contrast to most other applications of ^{14}C, levels in biomedical samples are many times modern levels because the doses given to the laboratory animals must be sufficient to swamp the natural signal. It is often necessary, in fact, to dilute the samples with 'dead' carbon in order to avoid contamination by very high levels of ^{14}C which might prejudice subsequent measurements of lower-level samples. Inevitably, however, because the starting material is many orders of magnitude above modern levels, there will be unexpectedly high uptakes from time to time, or mistakes in protocol, leading to samples which may be orders of magnitude higher than modern. The procedures must therefore be robust enough to cope with the occasional rogue sample. At the sample preparation stage, this is achieved by ensuring that everything with which the samples come in contact is disposable. Cross-contamination in the ion source is minimized by making its geometry as open as possible to ensure optimal pumping and by arranging that material sputtered from the samples is deposited on surfaces from which it is not readily remobilized. Nevertheless, if a particularly high-level sample is

encountered, it is generally necessary to clean the ion source before non-biomedical samples can be measured again.

Several AMS systems dedicated to biomedical applications of ^{14}C are being proposed (Purser 1994, Hughey *et al* 1997a, Mous 1997). In such systems, it is possible to relax the requirement that the charge state after stripping in the high-voltage terminal should be 3^+ or greater. Suter *et al* (1997) and Hughey *et al* (1997b) have independently demonstrated that essentially all of the potentially troublesome ^{13}CH and ^{12}CH$_2$ molecular ions can be dissociated in stripping to the 2^+ or even the 1^+ charge state by using either a long gas stripper or two sequential foil strippers at accelerating voltages as low as 0.5 MV. Hence, it is possible to contemplate the use of lower accelerating voltages than the 2–3 MV presently used by dedicated ^{14}C machines, with a corresponding reduction in size and cost. In parallel, ion source developments can be anticipated in which the AMS system is coupled directly to analysis systems such as gas or high-pressure liquid chromatographs, allowing on-line analysis of the various molecular components of a biomedical sample.

4.10.2. ^{26}Al.   The toxicity of aluminium has been firmly established for nearly 20 years, but the biochemistry of aluminium is still very imperfectly understood. This is a consequence of a number of factors. First, stable aluminium is mono-isotopic which rules out the use of stable isotopes as tracers. Secondly, the radioactive isotopes are either very long or short lived, making radioactive tracer studies impractical. Finally, concentrations of aluminium are extremely low in biological systems (1 ppm in tissues and 1 ppb in blood), whereas aluminium is prevalent in the environment where it constitutes 9% of the earth's crust. Hence, conventional chemistry is difficult and the possibility of contamination ever present.

The long-lived nature of ^{26}Al is, however, an opportunity for AMS. Because the specific activity is so low, it is possible to give doses of $\sim 10^{15}$ atoms (~ 50 ng) to human volunteers without a significant impact on their body burden of radiation. AMS is readily able to detect 10^6 atoms, which opens the way to long-term studies utilizing urine or small blood samples. The sample preparation and AMS methodologies for biomedical samples have been covered by King *et al* (1997a). Studies using human subjects include:

- The early biokinetics and long-term retention of aluminium injected as citrate (Priest *et al* 1995, Talbot *et al* 1995). Figure 17 shows the long-term excretion by a human subject of an injected dose of ^{26}Al.
- The distribution of aluminium among the various components of blood (Day *et al* 1991, 1994).
- Absorption from the gut and its dependence on the chemical form (soluble or insoluble) of the ingested aluminium (Priest *et al* 1996).
- The influence of co-administered silicate (Edwardson *et al* 1993, King *et al* 1997).
- The kinetics of aluminium absorption and excretion in both normal and renally-impaired subjects (Hohl *et al* 1994, Kislinger *et al* 1997a).
- Aluminium absorption rates in a group of Downs Syndrome patients (Moore *et al* 1997).

There have also been a number of animal and cell-culture studies. Meirav *et al* (1990) studied aluminium kinetics in rats, and there have been several studies in rats of the uptake of aluminium to the brain (Kobayashi *et al* 1990b, Fink *et al* 1994, Walton *et al* 1995, Yumoto *et al* 1997), as well as to other organs (Jouhanneau 1996, Barker *et al* 1997). In a culture study using human neuroblastoma cells, King *et al* (1994) found that neither DNA nor RNA were associated with aluminium, and that the distribution of aluminium in the cells was consistent with simple diffusion from the culture medium into the cells.
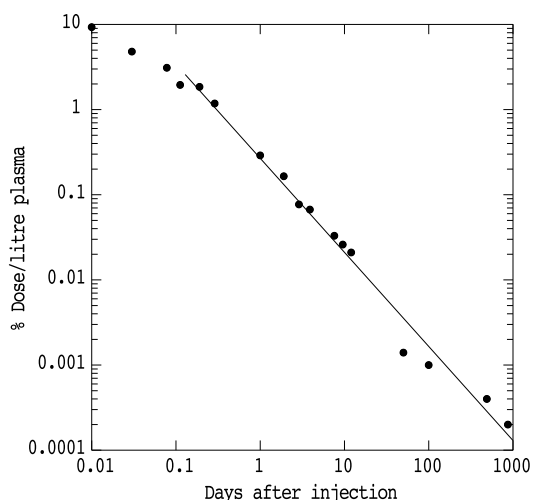
Figure 17. ^{26}Al in blood plasma for 1000 days following the injection of a dose of aluminium citrate containing 0.7 μg of ^{26}Al, determined by AMS (after Priest *et al* 1995). Note that the vertical scale extends over five orders of magnitude.

Aluminium is toxic to plants, and Johnson *et al* (1997) have demonstrated the feasibility of using ^{26}Al as a tracer to unravel the mechanism of this toxicity.

4.10.3. ^{41}*Ca.* Calcium-41 has potential in the study of bone loss, particularly in post-menopausal women. Unlike aluminium, calcium has a number of stable isotopes plus a radioactive isotope with a half-life of about a year. Nevertheless, ^{41}Ca offers a considerable gain in sensitivity over the former, and lower radiation dose coupled with longer-term sensitivity compared to the latter. Two studies to date have investigated the long-term labelling of the stable bone pool in human female subjects (Johnson *et al* 1994, Freeman *et al* 1997).

In another proof-of-principle study, using rabbit hearts, Southon *et al* (1994) measured the effect of interruption of the blood flow to the heart on calcium uptake and deposition with a view to improving the understanding of the processes leading to irreversible cell damage.

4.10.4. ^{32}*Si.* Silicon-32 is comparatively short-lived, and AMS must compete with liquid scintillation counting. Nevertheless, AMS offers advantages in terms of throughput and sensitivity even for this isotope, and a first measurement of the uptake of silicon from the gut has been reported by Popplewell *et al* (1998).

4.11. Hydrology

Chlorine-36 is the principal AMS isotope used in hydrology, although ^{129}I and ^{14}C have also been employed. Hydrological systems are in general complex, and these isotopes should be seen as complements to the more conventional tools employed by the hydrologist, rather than being used in isolation. Chlorine-36 has found application in determining the ages of groundwater, in measuring recharge rates, in studying past climates, and in investigating the hydrology of nuclear waste analogues and potential waste-disposal sites. Useful reviews have been given by Bentley *et al* (1986a) Fabryka-Martin *et al* (1987) and Fontes and Andrews (1994).

Perhaps the classic example of the use of ^{36}Cl for the dating of groundwater is the study of Bentley *et al* (1986b) of the Great Artesian Basin of Australia. This study was subsequently extended by Torgerson *et al* (1991). ^{36}Cl/Cl ratios vary from $\sim$110 $\times$ 10^{-15} near recharge to less than 10 $\times$ 10^{-15} at discharge. If the difference is due to decay of ^{36}Cl, then a transit time through the basin of 1.2 Ma may be inferred, in rather good agreement with a hydrological model of the basin. The ^{36}Cl/Cl ratio can, however, be changed by processes other than the decay of ^{36}Cl. Additional chloride may be acquired by the dissolution of evaporites already present within the aquifer matrix or by the diffusion of higher salinity solutions from elsewhere. Both processes lead to a decrease in the ratio. An increase in the ratio may result from additional ^{36}Cl produced *in situ* by neutrons which are due directly or indirectly to decay of uranium and thorium in the aquifer matrix. Further, the ^{36}Cl/Cl ratio at recharge may not have been constant in time as the result of climatic changes or of variations in ^{36}Cl production (see section 4.2.4). Consequently, alternative interpretations of the data have been proposed by Andrews and Fontes (1993) and Mazor (1992), and subsequently disputed (Kellett *et al* 1993, Fontes and Andrews 1993, Phillips 1993, Mazor 1993). Data which have been interpreted in terms of exponential decay of ^{36}Cl and hence age of water have also been presented for the Milk River aquifer in Canada (Phillips *et al* 1986, Nolte *et al* 1990, 1991). A few ^{129}I measurements of Great Artesian Basin waters have been reported (Fabryka-Martin *et al* 1985) and provide an estimate of the pre-bomb atmospheric ^{129}I/I ratio.

Chlorine-36 measurements, usually in conjunction with major ion chemistry and oxygen and hydrogen isotope data, have been employed in studies of groundwater evolution and residence times in a wide range of formations. Davie *et al* (1989) investigated the geographical distribution of recharge to a large aquifer in southern Australia. Balderer and Synal (1997) have studied the processes affecting ^{36}Cl concentrations and ^{36}Cl/Cl ratios in several groundwater systems in Turkey. The hydrology of an industrial injection site in Tennessee has been investigated by Vourvopolous *et al* (1990). In addition, Fehn and coworkers (Fehn *et al* 1990, 1992, 1994, Liu *et al* 1997, Moran *et al* 1995) have made extensive use of ^{129}I, often accompanied by ^{36}Cl, to investigate the origins and residence times of hydrothermal fluids and oil-field brines.

In conjunction with measurements of Cl$^-$, Br$^-$ and noble-gas concentrations, ^{36}Cl in groundwater may be used to reconstruct paleoclimates in terms of past levels of rainfall and evaporation. Studies have been reported for aquifers in the UK (Andrews *et al* 1994) and in Texas (Stute *et al* 1993).

The interest in ^{36}Cl as a hydrological tracer and chronometer has stimulated attempts to define the input function, and several studies of ^{36}Cl in rainfall have been performed. Measurements have been made in Israel (Herut *et al* 1992), in the continental USA (Hainsworth *et al* 1994, Knies *et al* 1994), in Canada (Milton *et al* 1994a) and in Australia (Keywood *et al* 1998).

Nuclear weapons testing in the 1950's and 1960's injected a large excess of ^{36}Cl into the atmosphere (see section 4.2.4). This bomb pulse has proved a useful tracer of recent water movement. For example, Norris *et al* (1990) and Fabryka-Martin *et al* (1993) have found evidence for bomb-pulse ^{36}Cl at considerable depth at the proposed nuclear waste disposal site at Yucca Mountain in Nevada, indicating that there are fast flow paths for water through fractures in the rock. Phillips *et al* (1988), Scanlon *et al* (1990) Walker *et al* (1992) and Cook *et al* (1994) have identified the bomb pulse in the unsaturated soil zone. Under favourable circumstances, the depth at which the pulse is found can yield the modern-day recharge rate, but more often, and particularly in semi-arid areas where recharge rates are low and vegetation is particularly effective at utilising the available water, the ^{36}Cl has held up at the root zone. Evidence for retention and recycling of bomb-pulse ^{36}Cl in the biosphere has been presented in

a series of papers by the Chalk River group (Milton *et al* 1994b, 1997, Cornett *et al* 1996, 1997).

Both ^{36}Cl and ^{129}I have been used in studies of analogues of nuclear waste disposal sites, including the Stripa granite in Sweden (Fabryka-Martin *et al* 1989, Andrews *et al* 1986, 1989) and uranium ore bodies in Australia (Fabryka-Martin *et al* 1988) and China (Jiang *et al* 1994).

4.12. Extra-terrestrial material

Long-lived isotopes such as ^{10}Be, ^{14}C, ^{26}Al, ^{36}Cl, ^{41}Ca, and ^{59}Ni are produced in meteorites or on the moon's surface by the action of cosmic rays. Levels may be much higher than at the surface of the earth, but the amount of material available for study is generally small. Hence the high sensitivity and low detection limits of AMS make it a more universally applicable tool than radioactive-decay counting. In studies of meteorites, cosmogenic isotope data serve to:

- authenticate extraterrestrial material, establishing its non-terrestrial origin from the pattern of cosmogenic isotopes it contains
- determine the irradiation history of the body in space
- establish the time at which a given meteorite fell to earth.

A useful review of each of these functions, and of the role played by AMS in these studies has been given by Herzog (1994). A subsequent study of depth profiles of ^{26}Al, ^{10}Be and ^{36}Cl in the Canyon Diablo iron meteorite has been reported by Michlovich *et al* (1994). Nishiizumi *et al* (1989b) have used the terrestrial age of a meteorite found within ice in Antarctica to date the ice.

4.13. Nuclear physics

The measurement of half-lives of long-lived isotopes has been the principal application of AMS to nuclear physics, although Paul *et al* (1987b) demonstrated the feasibility of measuring extremely low nuclear cross sections by AMS. For half-life measurements, AMS is used to determine the number of atoms in a source, while the activity of the source is usually measured by scintillation counting.

Middleton *et al* (1993) used AMS to determine absolute ^{10}Be/^{9}Be ratios for two standards of known activity in order to resolve a 3σ discrepancy between the two most precise measurements of the ^{10}Be half-life (Hofmann *et al* 1987, Inn *et al* 1987). Their measurements support the value of 1.51 ± 0.05 Ma obtained by Hofmann *et al*.

Kutschera *et al* (1984) determined a value of 1.49 ± 0.27 Ma for the half-life of ^{60}Fe, while more recently the half-lives of ^{79}Se (1.1 ± 0.2 Ma, Jiang *et al* 1997) and ^{126}Sn (207 ± 21 ka, Gartenmann *et al* 1996, Haas *et al* 1996) have also been determined using the combination of AMS and liquid scintillation counting.

The half-life of ^{32}Si has had a chequered career. Early indirect methods based on the decrease with depth of ^{32}Si concentrations in ice or sediment cores pointed to a value of $\sim$250 a. Two early AMS measurements (Elmore *et al* 1980b, Kutschera *et al* 1980), which were in excellent agreement, indicated a much lower value around 105 a. Subsequently, Alburger *et al* (1986), who followed the decay of a ^{32}Si source over a period of about four years, reported a value of 172 ± 4 a which differs by more than three standard deviations from the AMS result. This discrepancy prompted two new AMS measurements which eliminated some of the uncertainties inherent in the earlier experiments (Hofmann *et al* 1990, Thomsen *et al* 1991). Nevertheless, the results, 133 ± 9 and 162 ± 12 years respectively, indicate that consensus has still not been reached.

Klein *et al* (1991) have exploited the decline in ^{41}Ca concentration relative to ^{36}Cl in meteorites of increasing terrestrial age to determine a value of 103 ± 7 ka for the half-life of
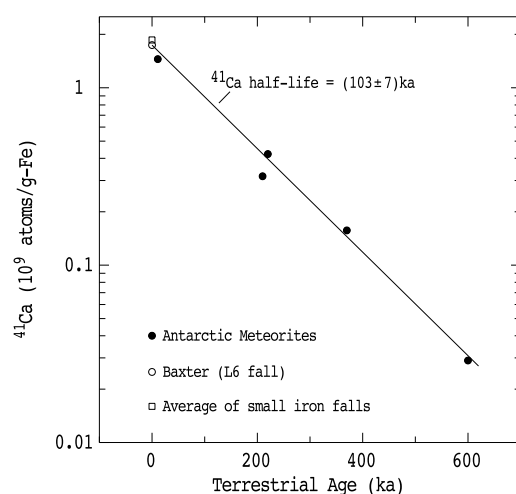
Figure 18. Determination of the half-life of ^{41}Ca from the relative concentrations of ^{41}Ca and ^{36}Cl in Antarctic meteorites with a range of terrestrial ages (from Klein *et al* 1991).

^{41}Ca (see figure 18). Appropriate meteorites, which spanned 600 ka in terrestrial age, were selected on the basis of evidence from other cosmogenic nuclides that the original meteorites had been small and had sufficiently long irradiation times that the concentrations of ^{41}Ca and ^{36}Cl were in secular equilibrium before the meteorites fell to earth.

4.14. Materials analysis

The ultra-sensitivity of AMS can be exploited to measure not only long-lived radio-isotopes, but also ultra-trace concentrations of stable isotopes in minerals or semiconductors.

Rucklidge and co-workers (Rucklidge *et al* 1982, 1990, Kilius *et al* 1984, 1990) have pioneered the measurement down to sub-ppb levels of platinum group elements directly in mineral grains in order to determine the partitioning between sulphide and silicate components for both commercial and research purposes. Samples are prepared as polished thin-sections, and the various minerals on each sample probed with a 0.5 mm diameter Cs beam. This concept is being further elaborated by Sie *et al* (1997) using a Cs microbeam to improve the spatial resolution to ∼30 μm.

An AMS system specifically for studying impurities in semiconductors has been developed at the University of North Texas (McDaniel *et al* 1990, 1994, 1995, Datar *et al* 1997), following proof-of-principle measurements at Arizona (Anthony and Donahue 1987). The earlier measurements indicated that the Cs beam used to sputter the sample was a significant source of contamination. The North Texas system therefore incorporates magnetic mass analysis of the primary Cs$^+$ beam, and all beam-optical components are fabricated from high-purity silicon. AMS analysis of the secondary (sputtered) beam overcomes the problem of molecular interferences which limit the sensitivity of the widely used secondary ion mass spectrometry (SIMS) systems, while retaining the desirable depth-profiling feature of SIMS. This concept has also been pursued at Zurich (Ender *et al* 1997), although the implementation differs significantly. A commercial Cs sputter gun which utilizes a velocity filter and a small angular deflection (to suppress neutral particles) is used to produce a pure Cs$^+$ beam, and the entire environment of the target is plated with high-purity gold to reduce contamination of the extracted ion beam.

A chlorine-specific technique has been employed by Datar *et al* (1995) to study the diffusion of chlorine implanted in silicon wafers. After implantation, the wafers were irradiated by neutrons in a reactor in order to convert $\sim$0.02% of the ^{35}Cl atoms to ^{36}Cl. Depth profiles of ^{36}Cl were then determined by AMS.

5. Conclusions and prospects

In the 20 years since the first demonstration that ^{14}C could be detected at natural levels using a tandem van de Graaff accelerator as part of a mass spectrometer, the field of AMS has expanded into many areas of science. Despite its maturity, growth continues at a rapid pace, both in terms of new facilities and in the diversity of applications. Adoption of the comparatively new high-intensity multi-sample ion sources by most AMS laboratories is fuelling large increases in throughput as their operation becomes better understood. This in turn opens new possibilities, not only in the biomedical field, but also in other more traditional areas such as archaeology, landscape evolution and oceanography where the ability to handle larger numbers of samples increases the range of problems that can be tackled. It is these two features in particular, the push to higher throughput on the technical side, and continuing diversification on the applications side, which signal the vitality of accelerator mass spectrometry as it enters its third decade.

Acknowledgments

References

Alburger D E, Harbottle G and Norton E F 1986 *Earth Planet. Sci. Lett.* **78** 168
Aldahan A and Possnert G 1998 *Quat. Geochron.* **17** 1023
Andrews J N, Davis S N, Fabryka-Martin J, Fontes J C, Lehmann B E, Loosli H H, Michelot J L, Moser H, Smith B and Wolf M 1989 *Geochim. Cosmochim. Acta* **53** 1803
Andrews J N, Edmunds W M, Smedley P L, Fontes J C, Fifield L K and Allan G L 1994 *Earth Planet. Sci. Lett.* **122** 159
Andrews J N and Fontes J C 1993 *Water Resour. Res.* **29** 1871
Andrews J N, Fontes J C, Michelot J L and Elmore D 1986 *Earth Planet. Sci. Lett.* **77** 49
Anthony J M and Donahue D J 1987 *Nucl. Instrum. Methods* B **29** 77
Artigalas H, Debrun J L, Kilius L, Zhao X L, Litherland A E, Pinault J L, Fouillac C and Maggiore C J 1994 *Nucl. Instrum. Methods* B **92** 227
Balderer W and Synal H A 1997 *Nucl. Instrum. Methods* B **123** 387
Ballantyne C K, Stone J O and Fifield L K 1998 *Holocene* **8** 347
Bard E 1998 *Geochim. Cosmochim. Acta* **62** 2025
Bard E, Arnold M, Fairbanks R G and Hamelin B 1992 *Radiocarbon* **35** 191
Bard E, Arnold M, Maurice P, Duprat J, Moyes J and Duplessey J-C 1987 *Nature* **328** 791
Bard E, Fairbanks R G, Arnold M and Hamelin B 1993 *The Last Glaciation: Absolute and Radiocarbon Chronologies, NATO ASI Series vol 12* ed E Bard and W S Broecker p 103
Bard E, Hamelin B, Fairbanks R G and Zindler A 1990a *Nature* **345** 405
Bard E, Hamelin B, Fairbanks R G, Zindler A, Mathieu G and Arnold M 1990b *Nucl. Instrum. Methods* B **52** 461
Bard E, Raisbeck G M, Yiou F and Jouzel J 1997 *Earth Planet. Sci. Lett.* **150** 453
Barker J, Day J P, Aitken T W, Charlesworth T R, Cunningham R C, Drumm P V, Lilley J S, Newton G W A and Smithson M J 1990 *Nucl. Instrum. Methods* B **52** 540

Barker J, Templar J, King S J, Day J P, Bradbury M W B, Radunovic A, Ueda F, Raja K, Lilley J S and Drumm P V 1997 *Nucl. Instrum. Methods* B **123** 275

Baumgartner S, Beer J, Masarik J, Wagner G, Meynadier L and Synal H-A 1998 *Science* **279** 1330

Baumgartner S, Beer J, Suter M, Dittrich-Hannen B, Synal H-A, Kubik P, Hammer C and Johnsen S 1997b *J. Geophys. Res.* **102** 26 659

Baumgartner S, Beer J, Wagner G, Kubik P, Suter M, Raisbeck G M and Yiou F 1997a *Nucl. Instrum. Methods* B **123** 296

Beasley T M, Cecil L D, Sharma P, Kubik P W, Fehn U, Mann L J and Gove H E 1993 *Ground Water* **31** 302

Beasley T M, Elmore D, Kubik P W and Sharma P 1992 *Ground Water* **30** 539

Beer J *et al* 1990 *Nature* **347** 164

Beer J, Baumgartner S, Dittrich-Hannen B, Hauenstein J, Kubik P, Lukasczyk C, Mende W, Stellmacher R and Suter M 1994b *The Sun as a Variable Star: Solar and Stellar Irradiance Variations* (Cambridge: Cambridge University Press) p 291

Beer J, Johnsen S J, Bonani G, Finkel R C, Lanway H, Oeschger H, Stauffer B, Suter M and Wölfli W 1992 *The Last Deglaciation: Absolute and Radiocarbon Chronologies* ed E Bard and W S Broecker (Berlin: Springer) p 141

Beer J, Joos Ch F, Lukasczyk C, Mende W, Siegenthaler U and Stellmacher R 1994a *The solar engine and its influence on terrestrial atmosphere and climate, NATO ASI Series vol 25* ed E Nisme-Ribes p 221

Beer J, Shen C, Heller F, Liu T, Bonani G, Dittrich B, Suter M and Kubik P W 1993 *Geophys. Res. Lett.* **20** 57

Bennett C L, Beukens R P, Clover M R, Gove H E, Liebert R B, Litherland A E, Purser K H and Sondheim W E 1977 *Science* **198** 508

Bentley H W, Phillips F M and Davis S N 1986a *Handbook of Environmental Isotope Geochemistry, The Terrestrial Environment* (Amsterdam: Elsevier) vol 2, p 427

Bentley H W, Phillips F M, Davis S N, Habermehl M A, Airey P L, Calf G E, Elmore D, Gove H E and Torgerson T 1986b *Water Resour. Res.* **22** 1991

Bierman P and Gillespie A 1991 *Geology* **19** 641

Bierman P, Gillespie A, Caffee M and Elmore D 1995 *Geochim. Cosmochim. Acta* **59** 3779

Bierman P and Steig E 1996 *Earth Surf. Proc. Landforms* **21** 125

Bierman P and Turner J 1995 *Quat. Res.* **44** 378

Boaretto E, Berkovits D, Hollos G and Paul M 1990 *Nucl. Instrum. Methods* B **50** 280

Bonani G, Eberhardt P, Hofmann H J, Niklaus T H, Suter M, Synal H A and Wölfli W 1990 *Nucl. Instrum. Methods* B **52** 338

Bonani G, Ivy S D, Hajdas I, Niklaus T R and Suter M 1994 *Radiocarbon* **36** 247

Bonani G, Ivy S, Wölfli W, Broshi M, Carmi I and Strugnell J 1992 *Radiocarbon* **34** 843

Brenninkmeijer C A M, Manning M R, Lowe D C, Wallace G, Sparks R J and Volz-Thomas A 1992 *Nature* **356** 50

Broecker W S, Andree M, Klas M, Bonani G, Wölfli W and Oeschger H 1988 *Nature* **333** 156

Bronk C R and Hedges R E M 1990 *Nucl. Instrum. Methods* B **52** 322

Bronk-Ramsey C and Hedges R E M 1994 *Nucl. Instrum. Methods* B **92** 100

——1997 *Nucl. Instrum. Methods* B **123** 539

Brook E J, Brown E T, Ackert R P, Raisbeck G M and Yiou F 1995 *Geology* **23** 1063

Brook E J, Nesje A, Lehman S J, Raisbeck G M and Yiou F 1996 *Geology* **24** 207

Brown E T, Bourlès D L, Colin F, Raisbeck G M, Yiou F and Desgarceaux S 1995a *Geophys. Res. Lett.* **22** 703

Brown E T, Bourlès D L, Colin F, Sanfo Z, Raisbeck G M and Yiou F 1994 *Earth Planet. Sci. Lett.* **124** 19

Brown E T, Edmond J M, Raisbeck G M, Bourlès D L, Yiou F and Measures C I 1992 *Geochim. Cosmochim. Acta* **56** 1607

Brown E T, Edmond J M, Raisbeck G M, Yiou F, Kurz M D and Brook E J 1991 *Geochim. Cosmochim. Acta* **55** 2269

Brown E T, Stallard R F, Larsen M C, Raisbeck G M and Yiou F 1995b *Earth Planet. Sci. Lett.* **129** 193

Brown L, Klein J, Middleton R, Sacks I S and Tera F 1982 *Nature* **299** 718

Brown L, Pavich M J, Hickman R E, Klein J and Middleton R 1988 *Earth Surf. Proc. Landforms* **13** 441

Brown L, Stensland G J, Klein J and Middleton R 1989 *Geochim. Cosmochim. Acta* **53** 135

Cerling T E and Craig H 1994 *Ann. Rev. Earth Planet. Sci.* **22** 273

Cini Castagnoli G *et al* 1995 *Geophys. Res. Lett.* **22** 707

Clark D H, Bierman P R and Larsen P 1995 *Quat. Res.* **44** 367

Clottes J *et al* 1995 *C.R. Acad. Sci., Paris* **320** 1133

Clottes J, Courtin J, Valladas H, Cachier H, Mercier N and Arnold M 1992 *Bulletin de la Société Préhistorique Française* **89** 270

Conard N J, Elmore D, Kubik P W, Gove H E, Tubbs L E, Chrunyk B A and Wahlen M 1986 *Radiocarbon* **28** 556

Cook P G, Jolly I D, Leaney F W, Walker G R, Allan G L, Fifield L K and Allison G B 1994 *Water. Resour. Res.* **30** 1709

Cornett R J *et al* 1996 *Water. Resour. Res.* **32** 1511

Cornett R J, Andrews H R, Chant L A, Davies W G, Greiner B F, Imahori Y, Koslowsky V T, Kotzer T, Milton J C D and Milton G M 1997 *Nucl. Instrum. Methods* B **123** 378

Cuffey K M and Clow G D 1997 *J. Geophys. Res.* **102** 26 383

Currie L A, Eglinton T I, Benner B A and Pearson A 1997 *Nucl. Instrum. Methods* **B123** 475

Currie L A, Klouda G A, Klinedinst D B, Sheffield A E, Jull A J T, Donahue D J and Connolly M V 1994 *Nucl. Instrum. Methods* B **92** 405

Damon P E *et al* 1989 *Nature* **337** 611

Dansgaard W *et al* 1993 *Nature* **364** 218

Datar S, Gove H E, Teng R D T and Lavine J P 1995 *Nucl. Instrum. Methods* B **99** 549

Datar S, Renfrow S N, Guo B N, Anthony J M, Zhao Z Y and McDaniel F D 1997 *Nucl. Instrum. Methods* B **123** 571

Davie R F, Kellett J R, Fifield L K, Evans W R, Calf G E, Bird J R, Topham S and Ophel T R 1989 *BMR J. Aust. Geol. Geophys.* **11** 261

Day J P, Barker J, Evans L J A, Perks J, Seabright P J, Ackrill P, Lilley J S, Drumm P V and Newton G W A 1991 *Lancet* **337** 1345

Day J P *et al* 1994 *Nucl. Instrum. Methods* B **92** 463

Dep L, Elmore D, Fabryka-Martin J, Masarik J and Reedy R C 1994a *Nucl. Instrum. Methods* B **92** 321

Dep L, Elmore D, Lipschutz M, Vogt S, Phillips F M and Zreda M 1994b *Nucl. Instrum. Methods* B **92** 301

Donahue D J *et al* 1997 *Nucl. Instrum. Methods* B **123** 51

Dorn R I and Phillips F M 1991 *Phys. Geography* **12** 303

Duplessey J-C, Arnold M, Maurice P, Bard E, Duprat J and Moyes J 1986 *Nature* **320** 350

Edwards R L, Beck J W, Burr G S, Donahue D J, Chappell J M A, Bloom A L, Druffel E R M and Taylor F W 1993 *Science* **260** 962

Edwardson J A, Moore P B, Ferrier I N, Lilley J S, Newton G W A, Barker J, Templar J and Day J P 1993 *Lancet* **342** 211

Eisma R, van der Borg K, de Jong A F M, Kieskamp W M and Veltkamp A C 1994 *Nucl. Instrum. Methods* B **92** 410

Elmore D *et al* 1980a *Nature* **286** 138

Elmore D, Anantaraman N, Fulbright H W, Gove H E, Hans H S, Nishiizumi K, Murrell M T and Honda M 1980b *Phys. Rev. Lett.* **45** 589

Elmore D, Conard N J, Kubik P W, Gove H E, Wahlen M, Beer J and Suter M 1987 *Nucl. Instrum. Methods* B **29** 207

Elmore D, Fulton B R, Clover M R, Marsden J R, Gove H E, Purser K H, Kilius L R, Beukens R and Litherland A E 1979 *Nature* **277** 22

Elmore D and Phillips F M 1987 *Science* **236** 543

Elmore D, Tubbs L E, Newman D, Ma X Z, Finkel R, Nishiizumi K, Beer J, Oeschger H and Andree M 1982 *Nature* **300** 735

Ender R M, Döbeli M, Suter M and Synal H A 1997 *Nucl. Instrum. Methods* B **123** 575

Etheridge D M, Steele L P, Langenfelds R L, Francey R J, Barnola J-M and Morgan V I 1996 *J. Geophys. Res.* **101** 4115

Evans J M, Stone J O H, Fifield L K and Cresswell R G 1997 *Nucl. Instrum. Methods* B **123** 334

Fabryka-Martin J, Bentley H, Elmore D and Airey P L 1985 *Geochim. Cosmochim. Acta* **49** 337

Fabryka-Martin J, Davis S N and Elmore D 1987 *Nucl. Instrum. Methods* B **29** 361

Fabryka-Martin J, Davis S N, Elmore D and Kubik P W 1989 *Geochim. Cosmochim. Acta* **53** 1817

Fabryka-Martin J, Davis S N, Roman D, Airey P L, Elmore D and Kubik P W 1988 *Chem. Geol.* **72** 7

Fabryka-Martin J T, Wightman S J, Murphy W J, Wickham M P, Caffee M W, Nimz G J, Southon J R and Sharma P 1993 *FOCUS '93: Site Characterisation and Model Validation (Las Vegas, Nevada)*

Fehn U, Moran J E, Teng R D T and Rao U 1994 *Nucl. Instrum. Methods* B **92** 380

Fehn U, Peters E K, Tullai-Fitzpatrick S, Kubik P W, Sharma P, Teng R D T, Gove H E and Elmore D 1992 *Geochim. Cosmochim. Acta* **56** 2069

Fehn U, Tullai-Fitzpatrick S, Teng R D T, Gove H E, Kubik P W, Sharma P and Elmore D 1990 *Nucl. Instrum. Methods* B **52** 446

Felton J S 1990 *et al Nucl. Instrum. Methods* B **52** 517

Fifield L K, Allan G L, Stone J O H and Ophel T R 1994 *Nucl. Instrum. Methods* B **92** 85

Fifield L K, Clacher A P, Morris K, King S J, Cresswell R G, Day J P and Livens F R 1997 *Nucl. Instrum. Methods* B **123** 400

Fifield L K, Cresswell R G, di Tada M L, Ophel T R, Day J P, Clacher A P, King S J and Priest N P 1996 *Nucl. Instrum. Methods* B **117** 295

Fifield L K, Ophel T R, Allan G L, Bird J R and Davie R F 1990 *Nucl. Instrum. Methods* B **52** 233

Fifield L K, Ophel T R, Bird J R, Calf G E, Allison G B and Chivas A R 1987 *Nucl. Instrum. Methods* B **29** 114

Fink D, Klein J and Middleton R 1990b *Nucl. Instrum. Methods* B **52** 572

Fink D, Middleton R and Klein J 1990a *Nucl. Instrum. Methods* B **47** 79

Fink D, Walton J, Hotchkis M A C, Jacobsen G E, Lawson E M, Smith A M, Tuniz C and Wilcox D 1994 *Nucl. Instrum. Methods* B **92** 473

Finkel R C and Nishiizumi K 1997 *J. Geophys. Res.* **102** 26 699

Finkel R C and Suter M 1993 *Adv. Anal. Chem.* **1** 1

Fontes J C and Andrews J N 1993 *Appl. Geochem.* **8** 663

——1994 *Nucl. Instrum. Methods* B **92** 367

Freeman S P H T, King J C, Vieira N E, Woodhouse L R and Yergey A L 1997 *Nucl. Instrum. Methods* B **123** 266

Freeman S P H T, Serfass R E, King J C, Southon J S, Fang Y, Woodhouse L R, Bench G S and McAninch J E 1995 *Nucl. Instrum. Methods* B **99** 557

Freeman S P H T and Vogel J S 1995 *Mass Spectrometry Ion Proc.* **143** 247

Gartenmann P, Golser R, Haas P, Kutschera W, Suter M, Synal H A, Wagner M J M and Wild E 1996 *Nucl. Instrum. Methods* B **114** 125

Gislefoss J S, Nydal R, Donahue D J, Jull A J T and Toolin L T 1994 *Nucl. Instrum. Methods* B **92** 431

Goslar T *et al* 1995 *Nature* **377** 414

Gosse J C, Klein J, Evenson E B, Lawn B and Middleton R 1995a *Science* **268** 1329

Gosse J C, Evenson E B, Klein J, Lawn B and Middleton R 1995b *Geology* **23** 877

Gove H E 1996 *Relic, Icon or Hoax? Carbon Dating the Turin Shroud* (Bristol: IOP)

Granger D E, Kirchner J W and Finkel R C 1996 *J. Geol.* **104** 249

——1997 *Geology* **25** 107

Grootes P M, Stuiver M, White J W C, Johnsen S and Jouzel J 1993 *Nature* **366** 552

Haas P, Gartenmann P, Golser R, Kutschera W, Suter M, Synal H A, Wagner M J M, Wild E and Winkler G 1996 *Nucl. Instrum. Methods* B **114** 131

Hainsworth L J, Mignerey A C, Helz G R, Sharma P and Kubik P W 1994 *Nucl. Instrum. Methods* B **92** 345

Hajdas I, Ivy S D, Beer J, Bonani G, Imboden D, Lotter A F, Sturm M and Suter M 1993 *Climatic Dynamics* **9** 107

Hajdas I, Zolitschka B, Ivy S D, Beer J, Bonani G, Leroy S A G, Negendank J W, Ramrath M and Suter M 1995 *Quaternary Sci. Rev.* **14** 137

Hedges R E M 1984 *Nucl. Instrum. Methods* **220** 211

Hedges R E M, Housley R A, Bronk C R and van Klinken G J 1992 *Archaeometry* **34** 337

Heimsath A M, Dietrich W E, Nishiizumi K and Finkel R C 1997 *Nature* **388** 358

Heinemeier J, Hornshøj P, Nielsen H L, Rud N and Thomsen M S 1987 *Nucl. Instrum. Methods* B **29** 110

Henken-Mellies W U, Beer J, Heller F, Hsü K J, Shen C, Bonani G, Hofmann H J, Suter M and Wölfli W 1990 *Earth Planet. Sci. Lett.* **98** 267

Herut B, Starinsky A, Katz A, Paul M, Boaretto E and Berkovits D 1992 *Earth Planet. Sci. Lett.* **109** 179

Herzog G F 1994 *Nucl. Instrum. Methods* B **92** 478

Hofmann H J, Beer J, Bonani G, von Gunten H R, Raman S, Suter M, Walker R L, Wölfli W and Zimmerman D 1987 *Nucl. Instrum. Methods* B **29** 32

Hofmann H J, Bonani G, Suter M, Wölfli W, Zimmerman D and von Gunten H R 1990 *Nucl. Instrum. Methods* B **52** 544

Hohl C, Gerisch P, Korschinek G and Nolte E 1994 *Nucl. Instrum. Methods* B **92** 478

Hughen K A, Overpeck J T, Lehman S J, Kashgarian M, Southon J, Peterson L C, Alley R and Sigman D M 1998 *Nature* **391** 65

Hughey B J, Klinkowstein R E, Shefer R E, Skipper P L, Tannenbaum S R and Wishnok J S 1997a *Nucl. Instrum. Methods* B **123** 153

Hughey B J, Shefer R E, Klinkowstein R E, Zhao X L, Kieser W E and Litherland A E 1997b *Nucl. Instrum. Methods* B **123** 186

Inn K G W, Raman S, Coursey B M, Fasset J D and Walker R L 1987 *Nucl. Instrum. Methods* B **29** 27

Ivy-Ochs S, Schlüchter C, Kubik P W, Dittrich-Hannen B and Beer J 1995 *Geology* **23** 1007

Jiang Songsheng, Guo J, Jiang Shan, Li C, Cui A, He M, Wu S and Li S 1997 *Nucl. Instrum. Methods* B **123** 405

Jiang Songsheng, Jiang Shan, Guo H, Du S, Zhanru C, Guo Q and Zhao Y 1994 *Nucl. Instrum. Methods* B **92** 385

Johnson R R, Berkovitz D, Boaretto E, Gelbart Z, Ghelberg S, Meirav O, Paul M, Prior J, Sossi V and Venczel E 1994 *Nucl. Instrum. Methods* B **92** 483

Johnson R R, Glass A D M, Kronzucker H, Gelbart Z, Venczel E, Paul M, Berkovitz D, Catan A, Kashiv Y and Ghelberg S 1997 *Nucl. Instrum. Methods* B **123** 283

Jones G A, McNichol A P, von Reden K F and Schneider R J 1990 *Nucl. Instrum. Methods* B **52** 278

Jouhanneau P 1996 *PhD Thesis* Universitè Paris XI Orsay (unpublished)

Jull A J T, Donahue D J, Broshi M and Tov E 1995 *Radiocarbon* **37** 11

Kellett J R, Evans W R, Allan G L and Fifield L K 1993 *Appl. Geochem.* **8** 653

Keywood M J, Cresswell R G, Allan G L, Fifield L K, Ayres G and Chivas A R 1998 *J. Geophys. Res.* **103** 8281

Kilius L, Baba N, Garwan M A, Litherland A E, Nadeau M J, Rucklidge J C, Wilson G C and Zhao X L 1990 *Nucl. Instrum. Methods* B **52** 357

Kilius L R, Rucklidge J C and Litherland A E 1987 *Nucl. Instrum. Methods* B **29** 72

Kilius L R, Rucklidge J C, Wilson G C, Lee H W, Chang K H, Litherland A E, Keiser W E, Beukens R P and Gorton M P 1984 *Nucl. Instrum. Methods* B **5** 185

King S J *et al* 1997a *Nucl. Instrum. Methods* B **123** 254

King S J, Oldham C, Carling R J, Popplewell J F, Day J P, Fifield L K, Liu K and Cresswell R G 1997b *The Analyst* at press

King S J, Templar J, Miller R V, Day J P, Dobson C B, Itzhaki R F, Fifield L K and Allan G L 1994 *Nucl. Instrum. Methods* B **92** 469

Kislinger G, Steinhausen C, Alvarez-Brückmann M, Winklhofer C, Ittel T H and Nolte E 1997 *Nucl. Instrum. Methods* B **123** 259

Kitagawa H, Fukuzawa H, Nakamura T, Okamura M, Takemura K, Hayashida A and Yasuda Y 1995 *Radiocarbon* **37** 371

Kitagawa H and van der Plicht J 1998 *Science* **279** 1187

Klein J, Fink D, Middleton R, Nishiizumi K and Arnold J 1991 *Earth Planet. Sci. Lett.* **103** 79

Klein J, Middleton R and Tang H 1982 *Nucl. Instrum. Methods* **193** 601

Klein J, Middleton R, Xue S, Herzog G F, Masarik J and Reedy R C 1995 *Lunar Planetary Sci. Conf.* **26** 763

Knie K, Faestermann T and Korschinek G 1997 *Nucl. Instrum. Methods* B **123** 128

Knies D L and Elmore D 1994 *Nucl. Instrum. Methods* B **92** 134

Knies D L, Elmore D, Sharma P, Vogt S, Li R, Lipschutz M E, Petty G, Farrell J, Monaghan M C, Fritz S and Agee E 1994 *Nucl. Instrum. Methods* B **92** 340

Kobayashi K, Imamura M, Nagai H, Yoshida K, Ohashi H, Yoshikawa H and Yamashita H 1990a *Nucl. Instrum. Methods* B **52** 254

Kobayashi K, Yumoto S, Nagai H, Hosoyama Y, Imamura M, Masuzawa S, Koizumi Y and Yamashita H 1990b *Proc. Japan Acad., Ser. B* **66** 189

Korschinek G, Faestermann T, Kastel T, Knie K, Maier H J, Fernandez-Niello J, Rothenberger M and Zerle L 1994 *Nucl. Instrum. Methods* B **92** 146

Korschinek G, Morinaga H, Nolte E, Preisenberger E, Ratzinger U, Urban A, Dragovitsch P and Vogt S 1987 *Nucl. Instrum. Methods* B **29** 67

Koslowsky V T, Andrews H R, Davies W G and Murnaghan K 1997 *Nucl. Instrum. Methods* B **123** 144

Kubik P W, Elmore D, Hemmick T K, Gove H E, Fehn U, Teng R T D, Jiang S and Tullai S 1987 *Nucl. Instrum. Methods* B **29** 138

Kutschera W 1990 *Nucl. Instrum. Methods* B **50** 252

Kutschera *et al* 1984 *Nucl. Instrum. Methods* B **5** 430

Kutschera W, Ahmad I, Glagola B G, Pardo R C, Rehm K E, Berkovitz D, Paul M, Arnold J R and Nishiizumi K 1993 *Nucl. Instrum. Methods* B **73** 403

Kutschera W, Fink D, Paul M, Hollos G and Kaufman A 1988 *Phys. Scr.* **37** 310

Kutschera W, Henning W, Paul M, Smither R K, Stephenson E J, Yntema J L, Alburger D E, Cumming J B and Harbottle G 1980 *Phys. Rev. Lett.* **45** 592

Lal D 1988 *Ann. Rev. Earth Planet. Sci.* **16** 355

——1991 *Earth Planet. Sci. Lett.* **104** 424

Lal D and Peters B 1967 *Handbuch der Physik* **46** 551

Levcenko V A *et al* 1997 *Nucl. Instrum. Methods* B **123** 290

Levcenko V A, Francey R J, Etheridge D M, Tuniz C, Head J, Morgan V I, Lawson E and Jacobsen G 1996 *Geophy. Res. Lett.* **23** 3345

Liu B, Phillips F M, Fabryka-Martin J T, Fowler M M and Stone W D 1994 *Water Resour. Res.* **30** 3115

Liu X, Fehn U and Teng R D T 1997 *Nucl. Instrum. Methods* B **123** 356

Lorblanchet M, Labeau M, Vernet J L, Fitte P, Vallados H, Cachier H and Arnold M 1990 *Rock Art Res.* **7** 4

Lowe D C, Brenninkmeijer C A M, Manning M R, Sparks R J and Wallace G 1988 *Nature* **332** 522

Lowe D C, Wallace G and Sparks R J 1987 *Nucl. Instrum. Methods* B **29** 291

McAninch J E, Bench J S, Freeman S P H T, Roberts M L, Southon J R, Vogel J S and Proctor I D 1995 *Nucl. Instrum. Methods* B **99** 541

McAninch J E, Hainsworth L J, Marchetti A A, Leivers M R, Jones P R, Dunlop A E, Mauthe R, Vogel J S, Proctor I D and Straume T 1997 *Nucl. Instrum. Methods* B **123** 137

McDaniel F D, Anthony J M, Kirchoff J F, Marble D K, Kim Y D, Renfrow S N, Grannan E C, Reznik E R, Vizkelethy

G and Matteson S 1994 *Nucl. Instrum. Methods* B **89** 242

McDaniel F D, Anthony J M, Renfrow S N, Kim Y D, Datar S and Matteson S 1995 *Nucl. Instrum. Methods* B **99** 537

McDaniel F D, Matteson S, Weathers J L, Marble D K, Duggan J L, Elliott P S, Wilson D K and Anthony J M 1990 *Nucl. Instrum. Methods* B **52** 310

McHargue L R and Damon P E 1991 *Rev. Geophys.* **29** 141

McHargue L R, Damon P E and Donahue D J 1995 *Geophys. Res. Lett.* **22** 659

Mak J E, Brenninkmeijer C A M and Manning M R 1992 *Geophys. Res. Lett.* **19** 1467

Mazarik J and Reedy R C 1995 *Earth Planet. Sci. Lett.* **136** 381

Mazaud A, Laj C and Bender M 1994 *Geophys. Res. Lett.* **21** 337

Mazor E 1992 *Appl. Geochem.* **7** 351

Mazor E 1993 *Appl. Geochem.* **8** 659

Meirav O, Sutton R A L, Fink D, Middleton R, Klein J, Walker V R, Halabe A, Vetterli D and Johnson R R 1990 *Nucl. Instrum. Methods* B **52** 536

Michlovich E S, Vogt S, Masarik J, Reedy R C, Elmore D and Lipschutz M E 1994 *J. Geophys. Res.* **99** 23187

Middleton R, Brown L, Dezfouly-Arjomandy B and Klein J 1993 *Nucl. Instrum. Methods* B **82** 399

Middleton R and Klein J 1987a *Phil. Trans. R. Soc.* A **323** 121

——1987b *Proc. Workshop on Tech. Accel. Mass Spectrom (Oxford, England)*

Middleton R, Klein J, Raisbeck G M and Yiou F 1983 *Nucl. Instrum. Methods* **218** 430

Milton G M *et al* 1994a *Nucl. Instrum. Methods* B **92** 376

Milton J C D *et al* 1997 *Nucl. Instrum. Methods* B **123** 382

Milton J C D, Andrews H R, Chant L A, Cornett R J, Davies W G, Greiner B F, Imahori Y, Koslowsky V T, McKay J W and Milton G M 1994b *Nucl. Instrum. Methods* B **92** 440

Molnar P *et al* 1994 *J. Geol.* **102** 583

Monaghan M C and Elmore D 1994 *Nucl. Instrum. Methods* B **92** 357

Monaghan M C, Klein J and Measures C I 1988 *Earth Planet. Sci. Lett.* **89** 288

Monaghan M C, Krishnaswami S and Thomas J H 1983 *Earth Planet. Sci. Lett.* **65** 51

Monaghan M C, Krishnaswami S and Turekian K K 1986 *Earth Planet. Sci. Lett.* **76** 279

Monaghan M C, McKean J, Dietrich W and Klein J 1992 *Earth Planet. Sci. Lett.* **111** 483

Moore P B, Edwardson J A, Ferrier I N, Taylor G A, Lett D, Tyler S P, Day J P, King S J and Lilley J S 1997 *Biol. Psych.* **41** 488

Moran J E, Fehn U and Hanor J S 1995 *Geochim. Cosmochim. Acta* **59** 5055

Morris J D 1991 *Ann. Rev. Earth Planet. Sci.* **19** 313

Morris J D, Leeman W P and Tera F 1990 *Nature* **344** 31

Morris J D, Ryan J and Leeman W P 1993 *J. Volcan. Geotherm. Res.* **58** 345

Morris J D and Tera F 1989 *Geochim. Cosmochim. Acta* **53** 3197

Mous D J W, Purser K H, Fokker W, van den Broek R and Koopmans R B 1997 *Nucl. Instrum. Methods* B **123** 159

Muller R A 1977 *Science* **196** 489

Nelson D E, Korteling R G and Stott W R, 1977 *Science* **198** 507

Nishiizumi K, Finkel R C, Caffee M W, Southon J R, Kohl C P, Arnold J R, Olinger C T, Poths J and Klein J 1994 *8th Int. Conf. Geochron. Cosmochron. Isot. Geol.: US Geol. Surv. Circular* **1107** p 234

Nishiizumi K, Finkel R C and Kohl C P 1996 *J. Geophys. Res.* **101** 22 225

Nishiizumi K, Jull A J T, Bonani G, Suter M, Wölfli W, Elmore D, Kubik P W and Arnold J R 1989b *Nature* **340** 550

Nishiizumi K, Kohl C P, Arnold J R, Dorn R, Klein J, Fink D, Middleton R and Lal D 1993 *Earth Surf. Proc. Landforms* **18** 407

Nishiizumi K, Kohl C P, Arnold J R, Klein J, Fink D and Middleton R 1991a *Earth Planet. Sci. Lett.* **104** 440

Nishiizumi K, Kohl C P, Shoemaker E M, Arnold J R, Klein J, Fink D and Middleton R 1991b *Geochim. Cosmochim. Acta* **55** 2699

Nishiizumi K, Winterer E L, Kohl C P, Klein J, Middleton R, Lal D and Arnold J R 1989a *J. Geophys. Res.* **94** 17 907

Nolte E, Krauthan P, Heim U and Korschinek G 1990 *Nucl. Instrum. Methods* B **52** 477

Nolte E, Krauthan P, Korschinek G, Maloszewski P, Fritz P and Wolf M 1991 *Appl. Geochem.* **6** 435

Norris A E, Bentley H W, Cheng S, Kubik P W, Sharma P and Gove H E 1990 *Nucl. Instrum. Methods* B **52** 455

Ophel T R, Fifield L K, Catford W N, Orr N A, Woods C L, Harding A and Clarkson G P 1988 *Nucl. Instrum. Methods* A **272** 734

Paul M 1990 *Nucl. Instrum. Methods* B **52** 315

Paul M, Berkovits D, Cecil L D, Feldstein H, Hershkowitz A, Kashiv Y and Vogt S 1997 *Nucl. Instrum. Methods* B **123** 394

Paul M, Fifield L K, Fink D, Albrecht A, Allan G L, Herzog G and Tuniz C 1993 *Nucl. Instrum. Methods* B **83** 275

Paul M, Fink D and Hollos G 1987b *Nucl. Instrum. Methods* B **29** 393

Paul M, Fink D, Hollos G, Kaufman A, Kutschera W and Magaritz M 1987a *Nucl. Instrum. Methods* B **29** 341

Pavich M J, Brown L, Harden J, Klein J and Middleton R 1986 *Geochim. Cosmochim. Acta* **50** 1727

Pavich M J and Vidic N 1993 *Climate Change in Continental Isotopic Records, Geophysical Monograph (American Geophysical Union)* **78** 263

Perry M, Elmore D, Rickey F, Bhukunwala B and Chong E 1997 *Nucl. Instrum. Methods* B **123** 178

Phillips F M 1993 *Appl. Geochem.* **8** 643

Phillips F M, Bentley H W, Davis S N, Elmore D and Swanick G B 1986 *Water. Resour. Res.* **22** 1991

Phillips F M, Mattick J L, Duval T A, Elmore D and Kubik P W 1988 *Water. Resour. Res.* **24** 1877

Phillips F M, Zreda M G, Flinsch M R, Elmore D and Sharma P 1996 *Geophys. Res. Lett.* **23** 949

Phillips F M, Zreda M G, Smith S S, Elmore D, Kubik P W, Dorn R I and Roddy D J 1991 *Geochim. Cosmochim. Acta* **55** 2695

Phillips F M, Zreda M G, Smith S S, Elmore D, Kubik P W and Sharma P 1990 *Science* **248** 1529

Popplewell J, King S J, Day J P, Ackrill P, Fifield L K, Cresswell R G, di Tada M L and Liu K 1998 *J. Inorg. Biochem.* **69** 177

Priest N D, Newton D, Day J P, Talbot R J and Warner A J 1995 *Human Experimental Toxicology* **14** 287

Priest N D, Talbot R J, Austin J G, Day J P, King S J, Fifield L K and Cresswell R G 1996 *Biometals* **9** 221

Prinoth-Fornwagner R and Niklaus T H 1994 *Nucl. Instrum. Methods* B **92** 282

Purser K H 1994 *Nucl. Instrum. Methods* B **92** 201

Purser K H, Kilius L R, Litherland A E and Zhao X L 1996 *Nucl. Instrum. Methods* **113** 445

Purser K H, Liebert R B and Russo C J 1980 *Radiocarbon* **27** 794

Purser K H, Smick T H and Purser R K 1990 *Nucl. Instrum. Methods* B **52** 263

Raisbeck G M, Yiou F, Bourles D, Lestringuez J and Deboffle D 1984 *Nucl. Instrum. Methods* B **5** 175

Raisbeck G M, Yiou F, Bourles D, Lorius C, Jouzel J and Barkov N I 1987 *Nature* **326** 273

Raisbeck G M, Yiou F, Fruneau M, Loiseaux J M, Lieuvin M, Ravel J and Lorius C 1981 *Nature* **292** 825

Raisbeck G M, Yiou F, Jouzel J, Petit J R, Barkov N I and Bard E 1992 *The Last Deglaciation: Absolute and Radiocarbon Chronologies* ed E Bard and W S Broecker (Berlin: Springer) p 127

Rao U and Fehn U 1997 *Nucl. Instrum. Methods* B **123** 361

Roberts M L, Velsko C and Turteltaub K W 1994 *Nucl. Instrum. Methods* B **92** 459

Robinson C, Raisbeck G M, Yiou F, Lehman B and Laj C 1995 *Earth Planet. Sci. Lett.* **136** 551

Rucklidge J 1995 *Analyst* **120** 1283

Rucklidge J, Gorton M P, Wilson G C, Kilius L R, Litherland A E, Elmore D and Gove H E 1982 *Can. Mineral.* **20** 111

Rucklidge J, Kilius L and Fuge R 1994 *Nucl. Instrum. Methods* B **92** 417

Rucklidge J, Wilson G C and Kilius L R 1990 *Nucl. Instrum. Methods* B **52** 507

Scanlon B R, Kubik P W, Sharma P, Richter B C and Gove H E 1990 *Nucl. Instrum. Methods* B **52** 489

Schlosser P, Kromer B, Ekwurzel B, Bönisch G, McNichol A, Schneider R, von Reden K, Östlund H G and Swift J H 1997 *Nucl. Instrum. Methods* B **123** 431

Sharma P, Elmore D, Miller T and Vogt S 1997 *Nucl. Instrum. Methods* B **123** 347

Shen C, Beer J, Liu T, Oeschger H, Bonani G, Suter M and Wölfli W 1992 *Earth Planet. Sci. Lett.* **109** 169

Sie S H, Niklaus T R and Suter G F 1997 *Nucl. Instrum. Methods* B **123** 112

Southon J S, Bishop M S and Kost G J 1994 *Nucl. Instrum. Methods* B **92** 489

Southon J S, Nelson D E and Vogel J S 1990 *Nucl. Instrum. Methods* B **52** 370

Spindler K 1994 *Nucl. Instrum. Methods* B **92** 274

Steig E J, Polissar P J, Stuiver M, Grootes P M and Finkel R C 1996 *Geophys. Res. Lett.* **23** 523

Stone J O H, Allan G L, Fifield L K and Cresswell R G 1996a *Geochim. Cosmochim. Acta* **60** 679

Stone J O H, Allan G L, Fifield L K, Evans J M and Chivas A R 1994 *Nucl. Instrum. Methods* B **92** 311

Stone J O H, Ballantyne C and Fifield L K 1998b *Geology* **26** 587

Stone J O H, Evans J M, Fifield L K, Allan G L and Cresswell R G 1998a *Geochim. Cosmochim. Acta* **62** 433

Stone J, Lambeck K, Fifield L K, Evans J M and Cresswell R G 1996b *Geology* **24** 707

Strack E, Heisinger B, Dockhorn B, Hartmann F J, Korschinek G, Nolte E, Morteani G, Petitjean C and Neumaier S 1994 *Nucl. Instrum. Methods* B **92** 317

Straume T *et al* 1998 *Health Phys.*

Stuiver M, Long A, Kra R S and Devine J M eds. 1993 *Calibration 1993, Radiocarbon* **35** 1

Stute M, Clark J F, Phillips F M and Elmore D 1993 *Int. Symp. Applications of Isotope Techniques in Studying Past and Current Environmental Changes in the Hydrosphere and the Atmosphere* (Vienna: IAEA) p 259

Suter M 1990 *Nucl. Instrum. Methods* B **52** 211

Suter M, Balzer R, Bonani G and Wölfli W 1984a *Nucl. Instrum. Methods* B **5** 242

——1984b *Nucl. Instrum. Methods* B **5** 251

Suter M, Beer J, Bonani G, Hofmann H J, Michel D, Oeschger H, Synal H-A and Wölfli W 1987 *Nucl. Instrum. Methods* B **29** 211

Suter M, Jacob S and Synal H A 1997 *Nucl. Instrum. Methods* B **123** 148

Synal H-A, Beer J, Bonani G, Lukasczyk C and Suter M 1994 *Nucl. Instrum. Methods* B **92** 79

Synal H-A, Beer J, Bonani G, Suter M and Wölfli W 1990 *Nucl. Instrum. Methods* B **52** 483

Talbot R J, Newton D, Priest N D, Austin J G and Day J P 1995 *Human Experimental Toxicology* **14** 595

Tera F, Brown L, Morris J D, Sacks I S, Klein J and Middleton R 1986 *Geochim. Cosmochim. Acta* **50** 535

Thomsen M S, Heinemeier J, Hornshøj, Nielsen H L and Rud N 1991 *Nucl. Phys.* A **534** 327

Torgerson T, Habermehl M A, Phillips F M, Elmore D, Kubik P, Jones B G, Hemmick T and Gove H E 1991 *Water Resour. Res.* **27** 3201

Trull T W, Brown E T, Marty B, Raisbeck G M and Yiou F 1995 *Chemical Geology* **119** 191

Tuniz C, Bird J R, Fink D and Herzog G F 1998 *Accelerator Mass Spectrometry: 'Ultrasensitive Analysis for Global Science'* (Boca Raton, FL: CRC Press)

Valette-Silver J N, Brown L, Pavich M, Klein J and Middleton R 1986 *Earth Planet. Sci. Lett.* **80** 82

Valladas H, Cachier H, Maurice P, Bernaldo de Quiros F, Clottes J, Caldera Valdés V, Uzquiano P and Arnold M 1992 *Nature* **357** 68

Van Roijen J J, Bintanja R, van der Borg K, van den Broeke M R, de Jong A F M and Oerlemans J 1994 *Nucl. Instrum. Methods* B **92** 331

Voelker A H L, Sarnthein M, Grootes P M, Erlenkeuser H, Laj C, Mazaud A, Nadeau M-J and Schleisher M 1998 *Radiocarbon* **40** 517

Vogel J S and Turteltaub K W 1994 *Nucl. Instrum. Methods* B **92** 445

Vogel J S, Turteltaub K W, Felton J S, Gledhill B L, Nelson D E, Southon J R, Proctor I D and Davis J C 1990 *Nucl. Instrum. Methods* B **52** 524

Von Reden K F, McNichol A P, Peden J C, Elder K L, Gagnon A R and Schneider R J 1997 *Nucl. Instrum. Methods* B **123** 438

Vourvopolous G, Brahana J V, Nolte E, Korschinek G, Priller A and Dockhorn B 1990 *Nucl. Instrum. Methods* B **52** 451

Wagner M J M, Synal H A and Suter M 1994 *Nucl. Instrum. Methods* B **89** 266

Wagner M J M, Synal H A, Suter M and Debrun J L 1995 *Nucl. Instrum. Methods* B **99** 519

Wahlen M, Tanake N, Henry R, Deck B, Seglen J, Vogel J S, Southon J, Shemesh A, Fairbanks R and Broecker W 1989 *Science* **245** 286

Walker G R, Jolly I D, Stadter M H, Leaney F W, Davie R F, Fifield L K, Ophel T R and Bird J R 1992 *Isotope Techniques in Water Resources Development* (Vienna: IAEA) p 19

Walton J, Tuniz C, Fink D, Jacobsen G and Wilcox D 1995 *Neurotoxicology* **16** 187

Wang L, Ku T L, Luo S, Southon J R and Kusakabe M 1996 *Geochim. Cosmochim. Acta* **60** 109

Wohlfarth B, Björck S and Possnert G 1995 *Radiocarbon* **37** 347

Wölfli W 1990 *Nucl. Instrum. Methods* B **29** 1

Yiou F, Raisbeck G M, Baumgartner S, Beer J, Hammer C, Johnsen S, Jouzel J, Kubik P W, Lestringuez J, Stiévenard M, Suter M and Yiou P 1997 *J. Geophys. Res.* **102** 26 783

Yiou F, Raisbeck G M, Bourles D, Lestringuez J and Debofle D 1986 *Radiocarbon* **28** 198

Yiou F, Raisbeck G M, Zhou Z Q and Kilius L R 1994 *Nucl. Instrum. Methods* B **92** 436

You C-F, Lee T and Li Y-H 1989 *Chemical Geology* **77** 105

You C-F, Morris J D, Gieskes J M, Rosenbauer R, Zheng S H, Xu X, Ku T L and Bischoff J L 1994 *Geochim. Cosmochim. Acta* **58** 4887

Yumoto S, Nagai H, Imamura M, Matsuzaki H, Hayashi K, Masuda A, Kumazawa H, Ohashi H and Kobayashi K 1997 *Nucl. Instrum. Methods* B **123** 279

Zhao X L, Nadeau M J, Garwan M A, Kilius L R and Litherland A E 1994a *Nucl. Instrum. Methods* B **92** 258

Zhao X L, Nadeau M J, Kilius L R and Litherland A E 1994b *Nucl. Instrum. Methods* B **92** 249

Zoppi U 1993 *PhD Thesis* Diss. ETH no. 10373

Zoppi U, Kubik P W, Suter M, Synal H A, von Gunten H R and Zimmerman D 1994 *Nucl. Instrum. Methods* B **92** 142

Zreda M and Noller J S 1998 *Science* **282** 1097

Zreda M G, Phillips F M and Elmore D 1994 *Water Resour. Res.* **30** 3127

Zreda M G, Phillips F M, Elmore D, Kubik P W, Sharma P and R I Dorn 1991 *Earth Planet. Sci. Lett.* **105** 94

Zreda M G, Phillips F M, Kubik P W, Sharma P and Elmore D 1993 *Geology* **21** 57